

STUDY OF DIELECTRIC RELAXATION OF GRAPHENE OXIDE

Submitted by
SHIBANI NAYAK
Adm. No.: 13PHY/17

A Thesis submitted in partial fulfillment of the requirements for the award of
the degree of

M.Sc. in Physics under

Orissa University of Agriculture and Technology (O.U.A.T)



2019

Under the Guidance of
Dr (Mrs)Sushama Baag

&

Dr. ChhatrapatiParida

Asst. Prof. Dept. of PHYSICS



Department Physics

College Of Basic Science and Humanities
Orissa Universities of Agriculture and Technology
Bhubaneswar- 751003, Odisha

CERTIFICATE – I

*This is to certify that the thesis entitled, “**STUDY OF DIELECTRIC RELAXATION OF GRAPHENE OXIDE**” is submitted in partial fulfillment of the requirements for the award of the degree of **Master of Science in Physics** of the **Orissa University of Agriculture and Technology, Bhubaneswar**, is a faithful record of bona fide research work carried out by **SHIBANI NAYAK** under my guidance and supervision and that no part of this thesis has been submitted for any other degree or diploma or published in any form.*

It is further certified that the help and sources of information availed of during the course of study have been duly acknowledged.

Dr(Mrs) Sushama Baag :Chairperson

Dept. of Physics

Guide

CERTIFICATE – II

*This is to certify that the thesis entitled, “**STUDY OF DIELECTRIC RELAXATION OF GRAPHENE OXIDE**” submitted in partial fulfillment of the requirements for the award of the degree of **Master of Science in Physics** of the **Orissa University of Agriculture and Technology, Bhubaneswar**, is a faithful record of bona fide research work carried out by **SHIBANI NAYAK** under my guidance and supervision and that no part of this thesis has been submitted for any other degree or diploma or published in any form.*

It is further certified that the help and sources of information availed of during the course of study have been duly acknowledged.

Advisory Committee

1. **1.Dr(Mrs)Sushama Baag** *Asst. Professor, Dept. of Physics* *Chairperson*
College of Basic Science & Humanities
O.U.A.T, Bhubaneswar
2. *Dr. Chhatrapati Parida* *Member*
Asst. Professor, Dept. of Physics
College of Basic Science & Humanities
O.U.A.T, Bhubaneswar
3. *Dr. Manas Ranjan Acharya* *Member*
Professor, Dept. of Physics
College of Basic Science & Humanities,
O.U.A.T., Bhubaneswar

External Examiner

Signature: _____ Name: _____
Designation: _____
Address: _____

DECLARATION

*I hereby declare that the project work entitled "**STUDY OF DIELECTRIC RELAXATION OF GRAPHENE OXIDE**" submitted by me for the partial fulfillment of the master of science to the **CBSH, Orissa university of agriculture and technology, Bhubaneswar** is my own original work and has not been submitted earlier to OUAT or to any other institution for the fulfillment of the requirement for any course of study. I also declare that no chapters of this manuscript in whole or in part in lifted and incorporated in this report from any earlier work done by me or others.*

,Place:Bhubaneswar

Signature:

date :

Name: SHIBANI NAYAK

Roll No: 13PHY/17

ACKNOWLEDGEMENT

I express my sincere gratitude to Dr.(Mrs)Sushama Baag Asstprof,Dept. of Physics for constantly guiding me at every step.

I express my sincere gratitude to Dr. ChhatrapatiParida, Asstprof,Dept. of Physics for giving me an opportunity to work on this project. Without his active support and guidance, this thesis would not have been successfully completed.

I sincerely convey my gratitude to Mr. PinakiChatterjee, Mr Mausam kumar of LARPM , CIPET, Government of India for providing experimental facility to synthesize graphene oxides. I am also thankful to Prof. Dr. Lalatendu Mohanty“ “Department of physics”, KIIT University and Dr Bibhu Prasad Ratha “Department of chemistry”, KIIT University for providing LCR Meter for dielectric study.

I also thank Dr. ManasRanjanAcharya, Dept. of Physics , Head of Dept. of Physics for consistent support, guidance and help. I am highly indebted for their help.

I also thank Prof. (Dr.) Bikash Panda Director of C.B.S.H, for consistent support, guidance.

SHIBANI NAYAK

Department of Physics

College Of Basic Science and Humanities

O.U.A.T

Adm. No. :- **13PHY/17**

Abstract

Herein this present work graphene oxide(GO) and by its subsequent reduction using ascorbic acid reduced graphene oxide(RGO) are synthesized using Hummers method.. Go and RGO pellets are prepared using polyvinyl alcohol and characterized by XRD, FTIR and UV spectroscopy.The characterization results revealed presence of oxygen containing functional groups such as hydroxyl, carbonyl, carboxylic group in GO and the removal of these functional groups after treatment with ascorbic acid. The dielectric and impedance parameters of GO pellets has been studied in the frequency range 1 Hz to 1MHz and in the temperature range 30⁰C to 100 ⁰C.The result demonstrate giant dielectric permittivity of GO ($\sim 10^5$) with low loss at 1 Hz and at 30 °C, which is even very high compared to conventional dielectric materials such as $\text{CaCu}_3\text{Ti}_4\text{O}_{12}$ and perosvkites. The dielectric constant of GO decreases to 75 at frequency of 1MHz.The ac conductivity of our GO was calculated and found to be $4 \times 10^{-5} \text{ ohm}^{-1}\text{cm}^{-1}$ at 1Hz and $75 \times 10^{-5} \text{ ohm}^{-1}\text{cm}^{-1}$ at 1 MHz .The variation of dielectric constant, dielectric loss, ac conductivity of GO with varying frequency and varying temperature are assessed using dielectric spectroscopy. The role of functional groups, frequency and temperature are elucidated and discussed with regard to the high dielectric constant. The present findings suggest that the GO can be used for scaling advances high performance electronic devices and high dielectric-based electronic and energy storage devices.

Introduction

a. Overview

Dielectrics are the materials which have wide range of applications such as for fabricating microelectronic for large scale power applications and energy storage devices.¹ Dielectric materials with high permittivity and low losses are used in the capacitors to store more electrical energy.² For metal, relative permittivity is negative and charge placed on the surface dissipates faster whereas for dielectrics it is positive and charge placed on the surface dissipates slowly.

Electrical insulator materials which will prevent the flow of current in an electrical circuit are being used since from the beginning of the science and technology of electrical phenomena. Dielectrics are insulating materials that exhibit the property of electrical polarization; thereby they modify the dielectric function of the vacuum.

The first capacitor was constructed by Cunaeus and Mussachenbroek in 1745 which was known as Leyden jar [1]. The physical form and construction of practical capacitors vary widely and many capacitor types are in common use. Most capacitors contain at least two electrical conductors often in the form of metallic plates or surfaces separated by a dielectric medium. A conductor may be a foil, thin film, sintered bead of metal, or an electrolyte.

But there were no studies about the properties of insulating materials until 1837. Faraday published the first numerical measurements on these materials, which he called dielectrics [2]. He has found that the capacity of a condenser was dependent on the nature of the material separating the conducting surface. Materials commonly used as dielectrics include glass, Ceramic, plastic film, paper, mica and oxide layers. Unlike a resistor, an ideal capacitor does not dissipate energy.

This discovery encouraged further empirical studies of insulating materials aiming at maximizing the amount of charge that can be stored by a capacitor. Throughout most of the 19th

century, scientists searching for insulating materials for specific applications have become increasingly concerned with the detailed physical mechanism governing the behavior of these materials. In contrast to the insulation aspect, the dielectric phenomena have become more general and fundamental, as it has the origin with the dielectric polarization.

Mossotti [3, 4] and Clausius [5] have done a systematic investigation about the dielectric properties of materials. They attempted to correlate the specific inductive capacity, a macroscopic characteristic of the insulator introduced by Faraday [2] which is now popularly termed as dielectric constant with the microscopic structure of the material. Following Faraday in considering the dielectrics to be composed of conducting spheres in a non-conducting medium, Clausius and Mossotti succeeded in deriving a relation between the real part of the dielectric constant ϵ_r and the volume fraction occupied by the conducting particles in the dielectric.

In the beginning of 20th century, Debye [6] realized that some molecules had permanent electric dipole moments associated with them, and this molecular dipole moment is responsible for the macroscopic dielectric properties of such materials. Debye succeeded in extending the Clausius -Mossotti theory to take into account the permanent moments of the molecules, which allowed him and others to calculate the molecular dipole moment from the measurement of dielectric constant. His theory was later extended by Onsager [7] and Kirkwood [8, 9] and is in excellent agreement with experimental results for most of the polar liquids. Debye's other major contribution to the theory of dielectrics is his application of the concept of molecular permanent dipole moment to explain the anomalous dispersion of the dielectric constant observed by Drude [10]. For an alternating field, Debye deduced that the time lag between the average orientation of moments and the field becomes noticeable when the frequency of the field is within the same order of magnitude as the reciprocal relaxation time. This way the molecular relaxation process leads to the macroscopic phenomena of dielectric relaxation, i.e., the anomalous dispersion of the dielectric constant and the accompanying absorption of electromagnetic energy over certain range of frequencies

Debye's theory shows excellent agreement with the experiments for the polar liquids while the dielectric behavior for solids was found to be deviating considerably. Several

modifications and extensions of Debye's theory have been proposed to correct this. There are two major approaches in the extension of Debye's theory. The first approach, pioneered by Cole [11], Davidson [12] and Williams [13], interprets the non-Debye relaxation behavior of the material in terms of the superposition of an exponentially relaxing process, which then leads to a distribution of relaxation times. The second approach by Joncher [14] proposes that the relaxation behavior at the molecular level is intrinsically non-Debye-like due to the cooperative molecular motions.

After more than eighty years of development, the theory of dielectrics is still a active area for research. Understanding the behaviour of dielectric materials with the variations of field, temperature and frequency is of particular importance for present day electronics. Modern day electronics demand dielectric materials with narrowly defined properties tailored for particular applications.

Recent advances in wireless communication technologies have elevated the interest in materials with the unusual combination of properties like high dielectric constant, low dielectric loss and low values of temperature dependence of dielectric constant [15]. The constant need for miniaturization provides a continuing driving force for the discovery and the development of increasingly sophisticated materials to perform the same or improved function with decreased size and weight. The dielectric materials mentioned above are used as the basis for resonators and filterers for the microwaves carrying the desired information [16]. These materials are presently employed as bulk ceramics in microwave communication devices. They are not integrated into the microelectronics but are being used as discrete components. The need for better dielectrics with improved properties suitable for modern integrated manufacturing needs is the motivation behind the present study.

b.Motivation

“A pencil and dream can take you anywhere”. Literally, this is what Geim and his dedicated group did in 2004, by discovering GN sheets from Graphite using a simple Scotch tape technique. Graphene is a wonder super carbon with enough potential to revolutionize current scientific and

technological world. Graphene and its derivatives stands as the centre of attraction of research community and if bibliometrics are to be trusted, the quantity of research papers on graphene will continue to increase rapidly over the next few decades. With only few years of delay with respect to graphene [17], the interest on graphene oxide (GO) [18] has exponentially risen, as documented by the yearly number of peer-reviewed works published on this topic, which have passed from a few units in 2007 to some thousands in 2013 (data taken from Scopus). GO is a two dimensional material. It is the oxidized form of graphene, with O functional groups decorating the sp^2 C basal plane [19]. All its physical properties can be tuned from those of fully oxidized GO to, approximately, those of graphene by simply removing the functional groups from its surface. This process allows it to pass from an insulating material to a semi-metal. Due to the presence of the O functional groups, GO is also hydrophilic and it can be dispersed in water solution [20], contrary to graphene which is hydrophobic. The size of the GO flakes can be also tuned and varied from a few nm to mm [21]. The tunability of both its chemical composition and flakes size makes GO an appealing material in many fields: electronics (sensors and transparent conductive films), composites materials, clean energy devices, biology and medicine. With focus on such different research fields, several reviews have been reported in the literature [22–32]. In the present study we give an account of the fundamental characterization of GO and few proposed applications, which we believe are among the most promising ones.

c. Research objectives

The main objective of our research is to synthesize graphene oxide(GO) and reduced graphene oxide (RGO) in cost effective method. This work subsequently demonstrated the effectiveness of GO as a gigantic dielectric material. The objective of the research includes:

1. Synthesis of GO from graphite using Hummers method.

2. Reduction of GO by ascorbic acid to form reduced graphene oxide(RGO)
3. Characterization of GO and RGO by XRD, FTIR and UV spectroscopy.
4. Investigate the dielectric behavior of GO by varying frequency and temperature.

d. Thesis outline

The thesis is composed of five chapters.

The chapter 1 depicts about 3D graphite, how graphene is produced from graphite, history of graphene, different properties like chemical and electronic properties of graphene. Different forms of graphene like monolayer, bilayer etc are also discussed. Finally different applications of graphene are elaborated in this chapter. Chapter 1 also depicts about graphene oxide (GO) and how graphene oxide is derived from graphene. Various functional groups present in the GO are discussed. The detail chemical structure, properties and applications of graphene oxide are elaborated. Then reduction of GO to reduced graphene oxide(RGO) using different reducing agents are explained.

A theoretical discourse of dielectric constant, its complex behavior, dielectric loss, different types of polarization in general is given. Finally the theoretical study of dielectric behavior of graphene oxide in particular is elaborated in chapter 2.

Chapter 3 discusses about detail experimental procedures in synthesis of GO and RGO. Different characterization techniques like XRD, FTIR, UV spectroscopy, dielectric measurements are discussed in details.

The chapter 4 is devoted for the characterization of prepared GO pellets by various analytical techniques such as UV-Visible spectroscopy, powder X-ray diffraction(XRD), fourier transform infrared spectroscopy(FT-IR) and the obtained results are discussed in details. This chapter also enumerates about dielectric studies of GO, variation of dielectric constant, dielectric losses, ac conductivity with variation in frequency and temperature are discussed with proper reasoning.

The final and the 5th Chapter summarize the thesis and recommends for future work.

CHAPTER 1

Literature review

It's always risky to make broad assertions about history, but one of the few things that seems to hold true is that technological advances drive the course of civilization. Bronze and iron were so crucial to the spread of ancient societies that they have entire epochs named after them. With the rise of the American steel industry, railroad tracks spread from Atlantic to Pacific, metal veins that carried the blood of a nation. Silicon semiconductors enabled the growth of computers and the greatest surge in information technology since the printing press. These materials shaped the development of society, and helped determine which countries dominated international relations. Today, a new material has the potential to alter the future. Dubbed a “supermaterial,” graphene has researchers the world over scrambling to better understand it.

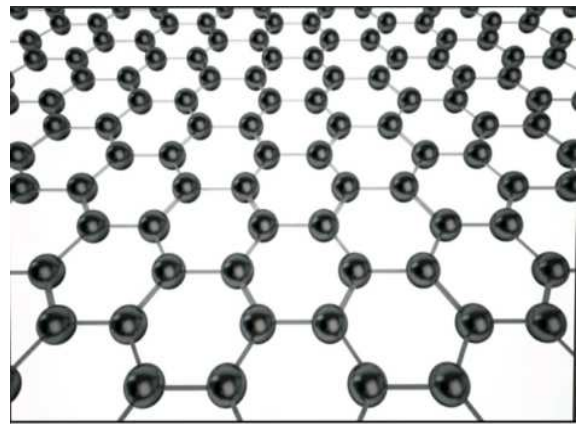


Fig1.1 Graphene's atoms are arranged in a honeycomb pattern.

The material's long list of superlative traits make it seem almost magical, but it could have very real and drastic implications for the future of physics and engineering. The simplest way to describe graphene is that it is a single, thin layer of graphite — the soft, flaky material used in pencil lead. Graphite is an allotrope of the element carbon, meaning it possesses the same atoms but they're arranged in a different way, giving the material different properties. For example, both diamond and graphite are forms of carbon, yet they have wildly different natures. Diamonds are incredibly strong, while graphite is brittle. Graphene's atoms are arranged in a hexagonal arrangement. Graphene has a theoretical specific surface area (SSA) of 2630 m²/g. This is much larger than that reported to date for carbon black (typically smaller than 900 m²/g) or for carbon nanotubes (CNTs), from ≈100 to 1000 m²/g and is similar to activated carbon.

Graphene is a crystalline allotrope of carbon with 2-dimensional properties. Its carbon atoms are densely packed in a regular atomic-scale chicken wire (hexagonal) pattern.

Each atom has four bonds, one σ bond with each of its three neighbours and one π -bond that is oriented out of plane. The atoms are about 1.42 Å apart.

Graphene's hexagonal lattice can be regarded as two interleaving triangular lattices. This perspective was successfully used to calculate the band structure for a single graphite layer using a tight-binding approximation.

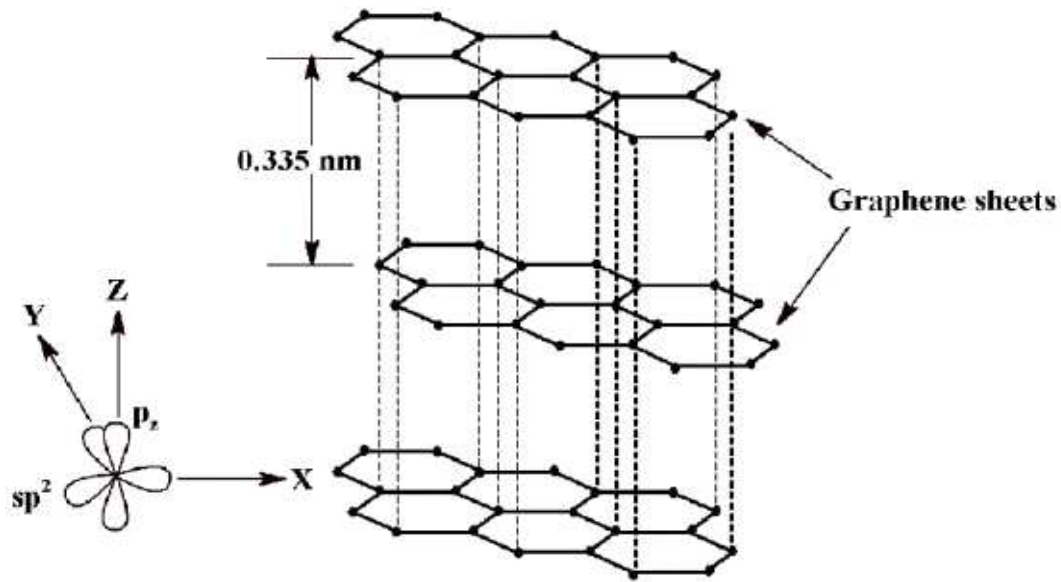


Fig 1.2 Layered structure of graphene showing sp^2 hybridisation

Graphene's stability is due to its tightly packed carbon atoms and a sp^2 orbital hybridization— a combination of orbitals s , p_x and p_y that constitute the σ -bond. The final p_z electron makes up the π -bond. The π -bonds hybridize together to form the π -band and π^* -bands. These bands are responsible for most of graphene's notable electronic properties, via the half-filled band that permits free-moving electrons.

Interestingly, when graphene is isolated from graphite it takes on some miraculous properties. It is a mere one-atom thick, the first two-dimensional material ever discovered. Despite this, graphene is also one of the strongest materials in the known universe. With a tensile strength of 130 GPa (gigapascals), it is more than 100 times stronger than steel.

Graphene's incredible strength despite being so thin is already enough to make it amazing, however, its unique properties do not end there. It is also flexible,

transparent, highly conductive, and seemingly impermeable to most gases and liquids. It almost seems as though there is no area in which graphene does not excel.

Today's graphene is normally produced using mechanical or thermal exfoliation, chemical vapour deposition (CVD), and epitaxial growth. One of the most effective way of synthesised graphene on a large scale could be by the chemical reduction of graphene oxide. Since the first report on mechanical exfoliation of monolayer graphene in 2004, interest in graphite oxide (which is produced by oxidation of graphite) has increased dramatically as people search for a cheaper, simpler, more efficient and better yielding method of producing graphene, that can be scaled up massively compared to current methods, and be financially suitable for industrial or commercial applications.

While graphite is a 3 dimensional carbon based material made up of millions of layers of graphene, graphite oxide is a little different. By the oxidation of graphite using strong oxidizing agents, oxygenated functionalities are introduced in the graphite structure which not only expand the layer separation, but also makes the material hydrophilic (meaning that they can be dispersed in water). This property enables the graphite oxide to be exfoliated in water using sonication, ultimately producing single or few layer graphene, known as graphene oxide (GO). The main difference between graphite oxide and graphene oxide is, thus, the number of layers. While graphite oxide is a multilayer system in a graphene oxide dispersion a few layers flakes and monolayer flakes can be found.

GO is a two dimensional material. It is the oxidized form of graphene, with O functional groups decorating the sp^2 C basal plane. All its physical properties can be tuned from those of fully oxidized GO to, approximately, those of graphene by simply removing the functional groups from its surface. This process allows it to pass from an insulating material to a semi-metal. Due to the presence of the O functional groups, GO is also hydrophilic and it can be dispersed in water solution, contrary to graphene which is hydrophobic. The size of the GO flakes can be also tuned and varied from a few nm to mm. The tunability of both its chemical composition and flakes size makes GO an appealing material in many fields: electronics (sensors and transparent conductive films), composites materials, clean energy devices, biology and medicine.

1.1. Synthesis and deposition of GO

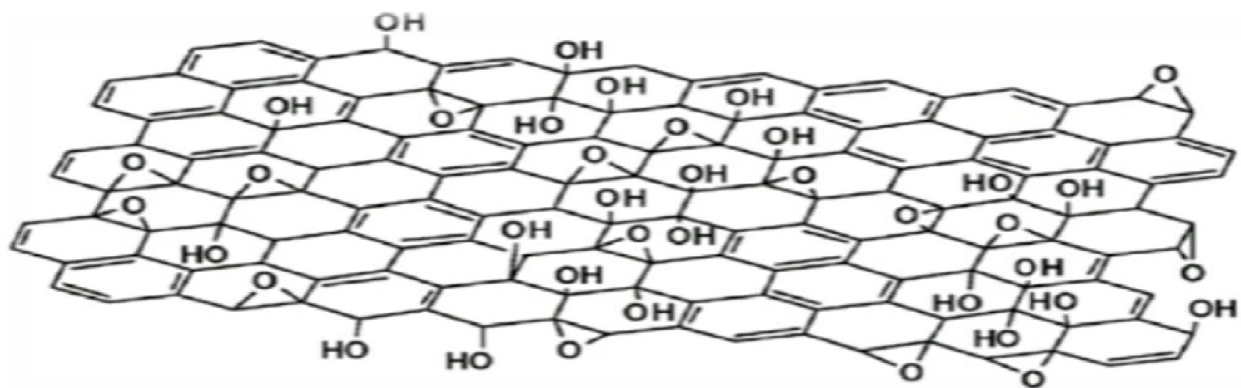


Fig 1.3 STRUCTURE OF GRAPHENE OXIDE

GO was firstly synthesized in 1859 by Sir 2nd Baronet Benjamin Collins Brodie, via oxidation of bulk graphite with potassium chlorate and nitric acid, but its chemical and structural nature has been studied only after more than a century by Lerf and Klinowsky through a careful analysis of solid-state C13 nuclear magnetic resonance (NMR) spectra. In their pioneering work, Lerf and Klinowsky propose that GO is built of non oxidized aromatic patches of variable size, which are separated from each other by aliphatic 6-membered rings containing hydroxyl groups, epoxide groups, and double bonds (figure 1.3). In this model, the O functional groups lie both above and below the basal plane, giving rise to the polar nature and hydrophilic behavior of GO.

Because of its hydrophilicity, graphite oxide is easily dispersed in water, where it breaks up into macroscopic atomically thin flakes, leading to solutions/suspensions of single layer GO. A typical GO solution has a brownish appearance, whose transparency and 'strength' is tuned by varying the solute concentration (figure 1.3).

Today, the most acknowledged method to synthesize GO is the modified Hummers method, which mainly consists of treating graphite with a mixture of sodium nitrate, potassium permanganate, and sulfuric acid. Even though GO is most commonly dispersed in water, it can be also in organic solvents,

where the GO sheets are negatively charged to become a colloidal suspension stabilized by electrostatic interactions.



Fig 1.4 GO SOLUTION

Synthesized GO can be deposited by drop casting, dip coating, spray coating, coating, Langmuir–Blodgett (LB) technique, and vacuum filtration. Uniform large area depositions can be achieved by spin coating or with the LB technique, which

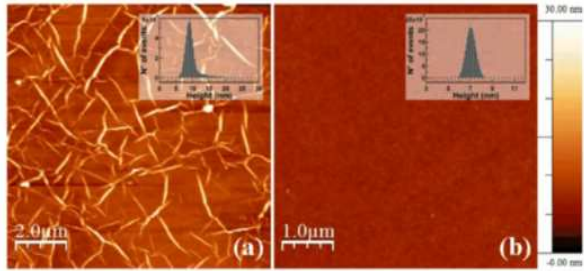


Fig 1.5:AFM images of 30 nm thick films of reduced GO deposited by spin coating (a)Nonsonicated GO(larger flakes)(b) Sonicated GO (smaller flakes)

allow to control the film thickness and to deposit thin films down to single-layer ones. If observed by atomic force microscopy (AFM), a typical GO film deposited by spin coating appears as in figure 1.4. The film (30 nm thick, in this case) has a roughness of 2 nm (root mean

square of the height distribution) and presents wrinkles on its surface (figure 1.5(a)), which disappear if the average

lateral size of the deposited flakes is smaller than few hundreds of nm (figure 1.5(b)).GO membranes, much thicker than the films prepared by spin coating or with the LB technique, can be obtained by vacuum filtration. In figure 1.6, the image of two of these membranes is reported.

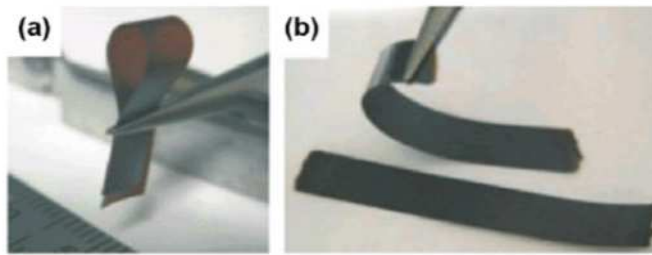


Fig 1.6:Photo of 5μm (a) and 25μm(b) thick GO membrane

1.2. Morphological properties

GO flakes are typically irregularly shaped. They have a lateral size ranging from few nanometers to some mm, depending on the domain size of the starting graphite, the oxidation time, and the type of oxidation procedure. Single layer GO flakes, with a lateral size of a few microns or more, can be easily observed by standard

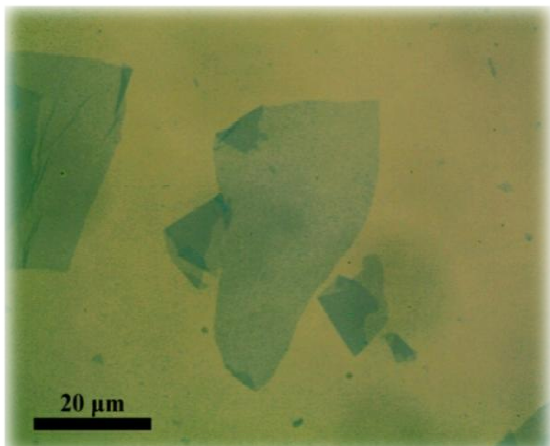


Fig 1.7OM image of GO deposited on 300nm SiO₂

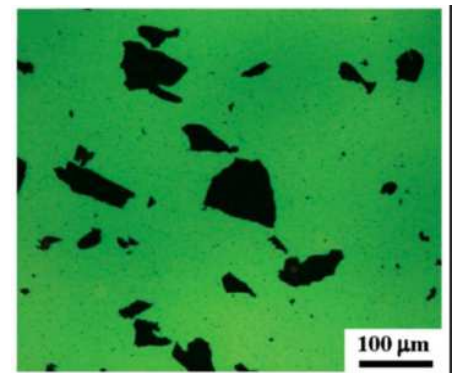


Fig 1.8 FM image of GO flakes on T4-functionalized 300 nm SiO₂/Si(1 0 0)

optical or fluorescence microscopy. Standard optical microscopy (OM) requires that GO is deposited on suitable dielectric substrates enhancing the optical contrast, such as those typically used for the optical identification of graphene, like 100 nm or 300 nm SiO₂/Si(1 0 0) or 72 nm Al₂O₃/Si(1 0 0) . An optical image of few dispersed single layer GO flakes (as correspondingly unequivocally determined with AFM height profiles) on 300 nm SiO₂/Si(1 0 0) is reported in figure 1.7. The presence of wrinkles (see, for example, the flake on the left part of figure 1.8) is a clear evidence of the conformational flexibility of GO. Due to this property, GO is often observed to be locally folded in double or multiple layers.

Given the ability of GO to quench fluorescence, fluorescence microscopy (FM) allows to further enhance the image contrast through the functionalization of the substrate with fluorescent molecules. In this case, the lateral resolution can be also improved and scaled even below the diffraction limit . An image of individual GO flakes quenching the fluorescence of T4-functionalized SiO₂ substrate is reported in figure 1.7.

The average lateral size of the GO flakes can be easily tuned by sonication, that reduces the dimensions of flakes by means of repeated fragmentation. In order to study the effects of sonication, scanning electron microscopy (SEM) can be profitably used, enabling large area (mm², useful for size statistics), high resolution (few nm), and good contrast imaging (folded regions can be also easily distinguished). SEM images of GO depositions with different size distributions are reported in figure 1.9 (panels (a)–(c)). The size of the GO flakes is reduced from panel (a) to panel (b) by increasing the sonication time. Fragmentation due to sonication can be quantitatively studied by processing the SEM images with a particle counter software. Morphological statistical analysis of 2 h sonicated GO is reported for example in figure 1.9. As typically occurring for random fragmentation processes the lateral size distribution is fitted by a log-normal model .This type of size distribution is independent on the sonication time . Once the size distribution is known, other important quantitative information can be derived, like the mass density probability distribution function, which allows to estimate the GO mass concentration in a specific size range.

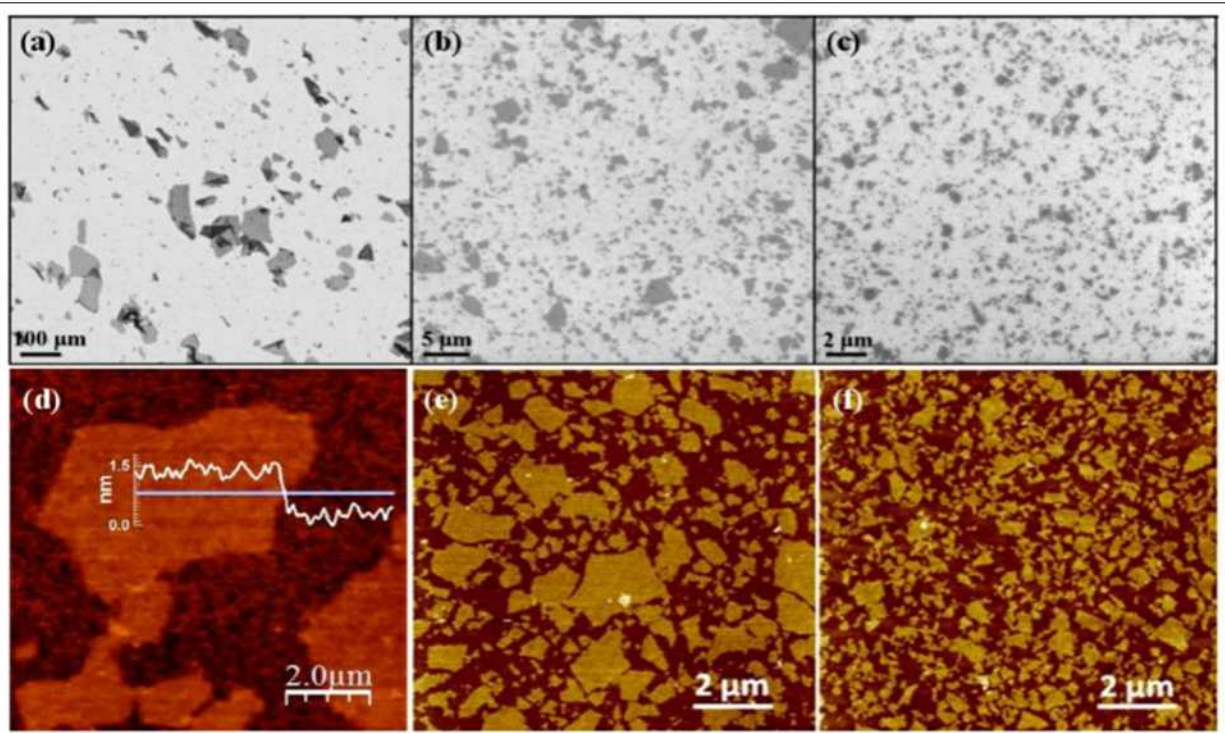


Fig1.9 SEM and AFM images of non-sonicated ((a) and (d)), 2 h sonicated ((b) and (e)), and 16 h sonicated ((c) and (f)) GO sheets deposited on SiO₂. Flakes are obtained from the same parent GO solution. Through the height profile reported in panel (d), a GO thickness of ~1.1 nm is measured.

Downscaling the microscopy techniques to the atomic resolution limit, one can obtain very detailed and useful structural and morphological information on GO and chemically modified reduced GO. This can be experimentally performed via

scanning tunneling microscopy (STM) or aberration-corrected transmission electron microscopy (TEM).

In the case of STM, the inherent need of a conductive sample favors the investigation of reduced GO flakes while pristine poorly conductive flakes are hardly imaged. In the first case, a very nicely STM experiment performed on GO monolayer is reported by Gomez-Navarro et al. (figure 1.10). On the flake surface it is clearly visible that the hexagonal lattice of the parent graphene structure (before oxidation) is partially preserved. However, the image is characterized also by patches of the surface where the ordered hexagonal lattice of graphene is lost.

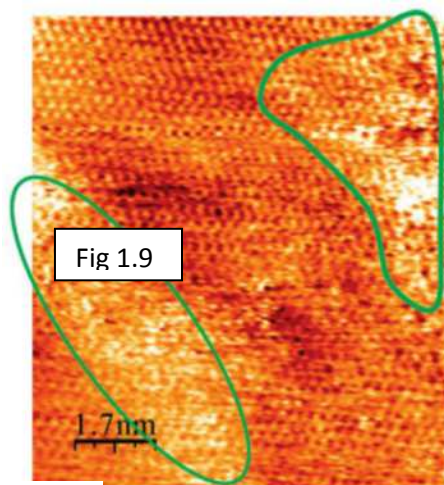


Fig 1.10 STM image of GO mono-layer deposited on highly ordered pyrolytic graphite. Oxidized regions are highlighted by green contour.

1.3 Graphene Oxide to Reduced Graphene Oxide

The exact process parameters used when reducing GO into RGO play a major role in the quality of the material, affecting how close a structure to perfect graphene is achieved.

If graphene is going to be adopted for large-scale applications such as energy storage, reduced graphene oxide could provide a suitable solution, since it is easier to manufacture in large quantities than perfect single-layer or few-layer graphene, and the quality will be sufficient for these bulk material applications.

The reduction of graphene oxide can be achieved a number of ways - through thermal, chemical, or electrochemical methods. The methods which are capable of producing the highest quality graphene tend to be more complex.

Some reported examples of graphene oxide reduction include:

1. treating graphene oxide with hydrazine hydrate at 100°C for 24 hours
2. exposure to hydrogen plasma for several seconds
3. exposure to powerful pulsed light from xenon flashtubes
4. heating the graphene oxide with urea as an expansion-reduction agent
5. direct heating of graphene oxide in a furnace to very high temperatures
6. Using chemical reduction to reduce GO is a scalable technique; however, the RGO produced by this method often has substandard electrical conductivity and surface area.

On the other hand, thermally reducing GO at above 1000°C produces a high surface area RGO which is similar to a pristine graphene. However, this process has a major drawback - the structure of the graphene platelets is damaged by the heating process, resulting in significant mass loss, and potentially impacting the mechanical strength of the RGO.

Electrochemical production of RGO could be the preferred commercial method used in the future, since it produced a material almost identical in structure to pristine graphene. In the electrochemical method, substrates like glass or indium tin oxide (ITO) are coated with a thin layer of graphene oxide. Electrodes are attached to each end of the substrate, and then linear sweep voltammetry is performed in a sodium phosphate buffer.

This method produces a very high quality material, and uses minimal harmful chemicals. However, it is difficult to scale, due to the need to deposit large quantities of GO on substrates.

1.4: Properties of Reduced Graphene Oxide

Properties of RGO are as follows:

- Reduction method: Chemically reduced
- Color: Black
- Form: Powder
- Odor: Odorless
- Sheet dimension: Variable
- Solubility: Insoluble
- Density: 1.91g/cm³
- Dispersability: It can be dispersed at low concentrations of less than 0.1mg/mL in DMSO, NMP, DMF
- Electrical conductivity: 666,7 S/m
- Humidity (Karl Fisher, TGA): 3.7 - 4.2%
- BET surface area: 422.69 – 499.85m²/g
- Elemental Analysis
- Oxygen (%): 13 – 22%
- Hydrogen (%): 0 – 1%
- Nitrogen (%): 0 – 1%
- Carbon (%): 77 – 87%
- Sulfur (%): 0

Applications

RGO is used in the following applications:

- Graphene research
- Batteries
- Biomedical
- Supercapacitors
- Printable graphene electronics

1.5.:Applications of GO

1.5.1:Optical nonlinearity[

Nonlinear optical materials are of great importance for ultrafast photonics and optoelectronics. Recently, the giant optical nonlinearities of graphene oxide (GO) has been proved useful for a number of applications. For example, the optical limiting of GO are indispensable to protect sensitive instruments from laser-induced damage. And the saturable absorption can be used for pulse compression, mode-locking and Q-switching. Also, the nonlinear refraction (Kerr effect) is crucial for functionalities including all-optical switching, signal regeneration, and fast optical communications.

One of the most intriguing and unique properties of GO is that its electrical and optical properties can be tuned dynamically by manipulating the content of oxygen-containing groups through either chemical or physical reduction methods. The tuning of the optical nonlinearities have been demonstrated during its entire laser-induced reduction process through continuous increase of the laser irradiance and four stages of different nonlinear activities have been discovered, which may serve as promising solid state materials for novel nonlinear functional devices. It is also proved that metal nanoparticles can greatly enhance the optical nonlinearity and [fluorescence](#) of graphene oxide.

1.5.2:Water purification[

Graphite oxides were studied for [desalination](#) of water using [reverse osmosis](#) beginning in the 1960s.^[52] In 2011 additional research was released.

In 2013 Lockheed Martin announced their [Perforene](#) graphene filter. Lockheed claims the filter reduces energy costs of reverse osmosis desalination by 99%. Lockheed claimed that the filter was 500 times thinner than the best filter then on the market, one thousand times stronger and requires 1% of the pressure. The product was not expected to be released until 2020.

Another study showed that graphite oxide could be engineered to allow water to pass, but retain some larger ions. Narrow capillaries allow rapid permeation by mono- or bilayer water. Multilayer laminates have a structure similar to [nacre](#), which provides mechanical strength at water free conditions. [Helium](#) cannot pass through the membranes in humidity free conditions, but penetrates easily when exposed to humidity, whereas water vapor passes with no resistance. Dry laminates are vacuum-tight, but immersed in water, they act as molecular sieves, blocking some solutes.

A third project produced graphene sheets with subnanoscale (0.40 ± 0.24 nm) pores. The graphene was bombarded with [gallium](#) ions, which disrupt carbon bonds. Etching the result with an oxidizing solution produces a hole at each spot struck by a gallium ion. The length of time spent in the oxidizing solution determined average pore size. Pore density reached 5 trillion pores per square centimeter, while retaining structural integrity. The pores permitted [cation](#) transport at short oxidation times, consistent with [electrostatic repulsion](#) from negatively charged [functional groups](#) at pore edges. At longer oxidation times, sheets were permeable to salt but not larger organic molecules.

In 2015 a team created a graphene oxide tea that over the course of a day removed 95% of heavy metals in a water solution

One project layered carbon atoms in a honeycomb structure, forming a hexagon-shaped crystal that measured about 0.1 millimeters in width and length, with subnanometer holes. Later work increased the membrane size to on the order of several millimeters.

Graphene attached to a polycarbonate support structure was initially effective at removing salt. However, defects formed in the graphene. Filling larger defects with nylon and small defects with hafnium metal followed by a layer of oxide restored the filtration effect.

In 2016 engineers developed graphene-based films that can filter dirty/salty water powered by the sun. Bacteria were used to produce a material consisting of two [nanocellulose](#) layers. The lower layer contains pristine [cellulose](#), while the top layer contains cellulose and graphene oxide, which absorbs sunlight and produces heat. The system draws water from below into the material. The water diffuses into the higher layer, where it evaporates and leaves behind any contaminants. The evaporate condenses on top, where it can be captured. The film is produced by repeatedly adding a fluid coating that hardens. Bacteria produce nanocellulose

fibers with interspersed graphene oxide flakes. The film is light and easily manufactured at scale.

1.5.3 :Coating

Optically transparent, multilayer films made from graphene oxide are impermeable under dry conditions. Exposed to water (or water vapor), they allow passage of molecules below a certain size. The films consist of millions of randomly stacked flakes, leaving nano-sized capillaries between them. Closing these nanocapillaries using chemical reduction with hydroiodic acid creates “reduced graphene oxide” (r-GO) films that are completely impermeable to gases, liquids or strong chemicals greater than 100 nanometers thick. Glassware or copper plates covered with such a graphene “paint” can be used as containers for corrosive acids. Graphene-coated plastic films could be used in medical packaging to improve shelf life.

1.5.4 Flexible rechargeable battery electrode

Graphene oxide has been demonstrated as a flexible free-standing battery anode material for room temperature lithium-ion and sodium-ion batteries. It is also being studied as a high surface area conducting agent in lithium-sulfur battery cathodes. The functional groups on graphene oxide can serve as sites for chemical modification and immobilization of active species. This approach allows for the creation of hybrid architectures for electrode materials. Recent examples of this have been implemented in lithium ion batteries, which are known for being rechargeable at the cost of low capacity limits. Graphene oxide-based composites functionalized with metal oxides and sulfides have been shown in recent research to induce enhanced battery performance. This has similarly been adapted into applications in supercapacitors, since the electronic properties of graphene oxide allow it to bypass some of the more prevalent restrictions of typical transition metal oxide electrodes. Research in this field is developing, with additional exploration into methods involving nitrogen doping and pH adjustment to improve capacitance. Additionally, research into reduced graphene oxide sheets, which display superior electronic properties akin to pure graphene, is currently being explored. Reduced graphene oxide applications greatly increases the conductivity and efficiency, while sacrificing some flexibility and structural integrity.

1.5.5:Energy Conversion

Photocatalytic Water Splitting is an artificial photosynthesis process in which water is dissociated into hydrogen (H₂) and oxygen (O₂), using artificial or natural light. Methods such as photocatalytic water splitting are currently being investigated to produce hydrogen as a clean source of energy. The superior electron mobility and high surface area of graphene oxide sheets suggest it may be implemented as a catalyst that meets the requirements for this process. Specifically, graphene oxide’s compositional functional groups of epoxide (-O-) and hydroxide (-OH) allow for more flexible control in the water splitting process. This flexibility can be used to tailor

the band gap and band positions that are targeted in photocatalytic water splitting. Recent research experiments have demonstrated that photocatalytic activity of graphene oxide containing a band gap within the required limits has produced effective splitting results, particularly when used with 40-50% coverage at a 2:1 hydroxide:epoxide ratio. When used in composite materials with CdS (a typical catalyst used in photocatalytic water splitting), graphene oxide nanocomposites have been shown to exhibit increased hydrogen production and quantum efficiency.

1.5.6 :Hydrogen Storage

Graphene oxide is also being explored for its applications in hydrogen storage. Hydrogen molecules can be stored among the oxygen-based functional groups found throughout the sheet. This hydrogen storage capability can be further manipulated by modulating the interlayer distance between sheets, as well as making changes to the pore sizes. Research in transition metal decoration on carbon sorbents to enhance hydrogen binding energy has led to experiments with titanium and magnesium anchored to hydroxyl groups, allowing for the binding of multiple hydrogen molecules.

CHAPTER 2

DIELECTRIC PROPERTIES

A theoretical discourse of dielectric constant, its complex behavior, dielectric loss, different types of polarization in general is given. Finally the theoretical study of dielectric behavior of graphene oxide in particular is elaborated.

2.1 Dielectric constant

2.1.1:What Is Dielectric Constant?

Dielectric constant is the ratio of the capacitance formed by two plates with a material between them to capacitance of the same plates with air as a dielectric.

2.1.2:How It Arises?

When an insulating material is placed in an electric field, it allows the electric lines of flux to enter inside it. As a result positively charged nucleus of an atom pushed in the direction of the field while negatively charged electrons pushed in the opposite direction of field. Thus polarization occurs, which is the main cause of development of dielectric constant.

2.1.3: Types of Dielectric Constant.

Dielectric constant arises due to polarization is of two type i.e. real dielectric constant (ϵ'_r) and imaginary part of dielectric constant (ϵ_r''). Imaginary part of dielectric constant also known as imaginary part of dielectric loss.

2.1.4: Dielectric Loss

Dielectric loss quantifies a dielectric material's inherent dissipation of electromagnetic energy .It can be parameterized in terms of either the loss angle δ or the corresponding loss tangent $\tan \delta$. Both refer to the phasor in the complex plane whose real and imaginary parts are the resistive (lossy) component of an electromagnetic field and its reactive (lossless) counterpart.

2.1.5 Ac Conductivity

It is a fundamental property of a material that quantifies how strongly it resists or conducts the flow of current . Generally it is the reciprocal of electrical resistivity . It represents a material's ability to conduct electric current. It is commonly signified by Greek letter ' σ '.

2.2:POLARISATION

2.2.1:What Is Polarization?

An insulator has low electrical conductivity because all the charges in insulator are in bound state. When electric field is applied to

an insulator, as it has no free charge like that of conductor, with the applied electric field +ve ly and –ve ly bound charges are separated. We can say that a dipole is created by atom of the insulator. This is known as polarization. Polarization in dielectrics is of four types.

2.2.2 Types of Polarization

2.2.2.1 Dipolar polarization

Dipolar polarization arises in those substances in which molecules have a permanent dipole moment. But in absence of electric field the net polarization vanishes due to random orientation of molecules. When electric field is applied the molecular dipole tends to align with the field and this result in a net non-vanishing polarization. This is called dipolar polarization.

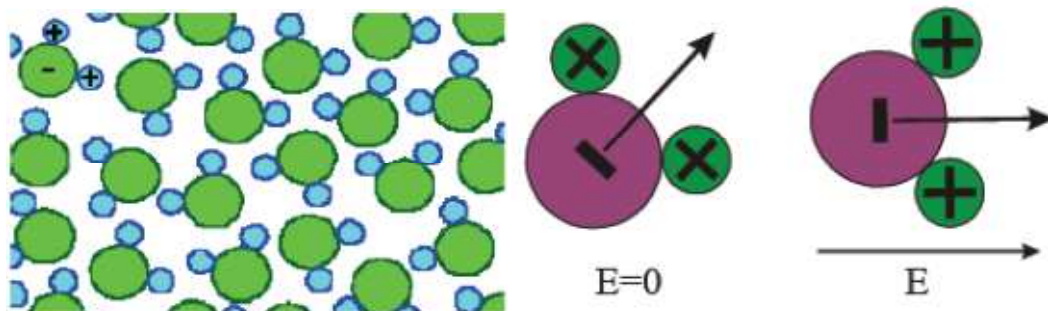


Fig2.1 : Orientation of dipoles in presence of electric field

2.2.2.2: Ionic polarization

If the molecule contains ionic bonds, then the field tends to stretch the lengths of these bonds. The effect of this change in length is to produce a net dipole moment in the unit cell where previously there was none. Since the polarization here is due to the relative displacements of oppositely charged ions, we speak of ionic polarisability.

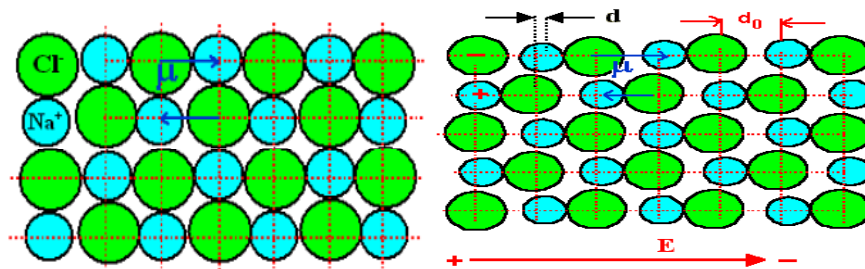


Fig2.2: Inter atomic distance changes due to ionic polarization

2.2.2.3: Electronic polarisability

This type of polarisability arises because of the individual atoms or ions in a molecule are themselves polarized by the field i.e. the electrons in its various shells are displaced with respect to the nucleus.

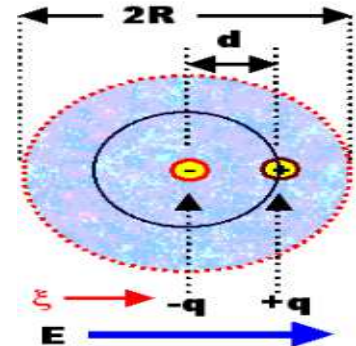


Fig2.3: Inter atomic distance changes due to electronic polarization

2.2.2.4 Interfacial Polarisation

This type of polarisability arises because of presence of some free charges in an insulator, but these are not responsible for conduction of current as their amount is very less. During polarization these free electrons appear at the interface of the dipoles. So this is called interfacial polarization.

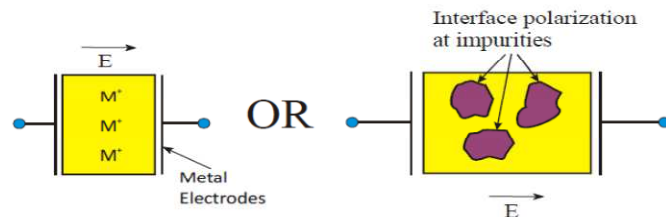


Fig2.4-Interfacial polarization

2.3 Frequency dependence of dielectric constant

In absence of electric field only force acting is restoring force.

$$F_{rest} = ma$$

$$\Rightarrow -m\omega_0^2 x = ma$$

$$\Rightarrow \omega_0^2 x + \frac{d^2 x}{dt^2} = 0 \quad (\omega_0 = \text{Natural frequency of oscillation})$$

Now in presence of electric field we can write

$$F = F_{rest} + F_{ext}$$

$$\Rightarrow a = \frac{F_{rest}}{m} + \frac{F_{ext}}{m}$$

$$\Rightarrow \frac{d^2 x}{dt^2} = -\omega_0^2 x + \frac{F_{ext}}{m}$$

$$\Rightarrow \frac{d^2 x}{dt^2} + \omega_0^2 x = \frac{F_{ext}}{m} = \frac{qE_0 e^{-i\omega t}}{m} \quad \text{-----(2.1)}$$

We have from the definition of dipole moment

$$p = qx$$

Where q =charge and x =distance between charges

If N be the number of dipoles per unit volume, then total number of dipoles will be, $Np=Nqx=P$

Multiplying equation (1) by Nq

$$\begin{aligned}
 Nq \frac{d^2x}{dt^2} + Nq\omega_0^2 x &= Nq \cdot \frac{qE_0 e^{-i\omega t}}{m} \\
 \Rightarrow \frac{d^2P}{dt^2} + \omega_0^2 P &= \frac{Nq^2 E_0 e^{-i\omega t}}{m} \\
 \Rightarrow \frac{d^2P}{dt^2} + \omega_0^2 P &= \frac{Nq^2 \epsilon_0 \omega_0^2 E}{m \epsilon_0 \omega_0^2} \\
 \Rightarrow \frac{d^2P}{dt^2} + \omega_0^2 P &= \chi_0 \epsilon_0 \omega_0^2 E \quad \text{-----(2.2)}
 \end{aligned}$$

Solution of equation(2) can be written as

$$P = P_0 e^{-i\omega t}$$

Putting this solution in equation (2.2)

$$\begin{aligned}
 \Rightarrow P_0 (-i\omega)^2 e^{-i\omega t} + \omega_0^2 P_0 e^{-i\omega t} &= \chi_0 \epsilon_0 \omega_0^2 E \\
 \Rightarrow -\omega^2 P + \omega_0^2 P &= \chi_0 \epsilon_0 \omega_0^2 E \\
 \Rightarrow P &= \frac{\chi_0 \epsilon_0 \omega_0^2 E}{\omega_0^2 - \omega^2} \\
 \Rightarrow P &= \left(\frac{\chi_0 \epsilon_0 \omega_0^2}{\omega_0^2 - \omega^2} \right) E \quad \text{-----(2.3)}
 \end{aligned}$$

From equation(2.3) it is clear that $P \propto E$

$$P = \epsilon_0 \chi(\omega) E$$

Where $\chi(\omega) = \frac{\chi_0 \omega_0^2}{\omega_0^2 - \omega^2}$

When $\omega \rightarrow \omega_0$

Then $\chi(\omega) = \infty$

But this is impossible. So there must be some resistive force

i.e. damping force, $F_{\text{damp}} \propto \frac{dx}{dt}$

$$\propto Nq \frac{dx}{dt}$$

$$\propto \frac{d(Nqx)}{dt}$$

$$\propto \frac{dP}{dt} = \sigma \frac{dP}{dt}$$

So total force

$$F = F_{\text{rest}} + F_{\text{ext}} + F_{\text{damp}}$$

$$\frac{d^2 P}{dt^2} + \omega_0^2 P + \sigma \frac{dP}{dt} = \chi_0 \epsilon_0 \omega_0^2 E \quad \text{-----(2.4)}$$

Now putting the solution in above equation

$$\Rightarrow (-i\omega^2)P + \sigma(-i\omega)P + \omega_0^2 P = \chi_0 \epsilon_0 \omega_0^2 E$$

$$\Rightarrow P = \frac{\chi_0 \epsilon_0 \omega_0^2 E}{\omega_0^2 - \omega^2 - i\sigma\omega}$$

$$\Rightarrow P = \left(\frac{\chi_0 \omega_0^2}{\omega_0^2 - \omega^2 - i\sigma\omega} \right) \epsilon_0 E \quad \text{-----} (2.5)$$

Where $\chi(\omega) = \frac{\chi_0 \omega_0^2}{\omega_0^2 - \omega^2 - i\sigma\omega}$

$$\frac{\chi(\omega)}{\omega_0^2 - \omega^2 + i\sigma\omega} = \frac{\chi_0 \omega_0^2}{\omega_0^2 - \omega^2 - i\sigma\omega} \times \frac{1}{\omega_0^2 - \omega^2 + i\sigma\omega}$$

$$\Rightarrow \frac{\chi(\omega)}{\omega_0^2 - \omega^2 + i\sigma\omega} = \frac{\omega_0^2 \chi_0}{(\omega_0^2 - \omega^2)^2 + (\sigma\omega)^2}$$

$$\Rightarrow \chi(\omega) = \frac{\omega_0^2 \chi_0 (\omega_0^2 - \omega^2)}{(\omega_0^2 - \omega^2)^2 + (\sigma\omega)^2} + \frac{i\omega_0^2 \chi_0 \sigma\omega}{(\omega_0^2 - \omega^2)^2 + (\sigma\omega)^2}$$

$$\Rightarrow \chi(\omega) = \chi'(\omega) + \chi''(\omega) \quad \text{-----} (2.6)$$

We have

$$\epsilon = \epsilon_0(1 + \chi)$$

$$= \epsilon_0(1 + \chi'(\omega) + i\chi''(\omega))$$

$$= \epsilon_0(1 + \chi'(\omega)) + i\epsilon_0\chi''(\omega)$$

$$= \epsilon'(\omega) + i\epsilon'' \quad \text{-----} (2.7)$$

Where, $\epsilon'(\omega) = \epsilon_0 \left[1 + \frac{\omega_0^2 \chi_0 (\omega_0^2 - \omega^2)}{(\omega_0^2 - \omega^2)^2 + (\sigma\omega)^2} \right]$

$$\epsilon'' = \frac{\epsilon_0 \omega_0^2 \chi_0 \sigma\omega}{(\omega_0^2 - \omega^2)^2 + (\sigma\omega)^2}$$

2.4 Dielectric loss

Dielectric relaxation is the lag in dipole orientation behind an alternating applied electric field. Under the influence of such a field the polar molecules of a system rotate towards an equilibrium distribution. When the polar molecules are large or the frequency of alternating field is high, the rotational motion of molecules is not sufficiently rapid for attainment of equilibrium with the field. The polarization then acquires a component out of phase with the field and the displacement current acquires a conductance component in phase with the field. This conductance component obeys ohms law and it results in thermal dissipation of energy.

In an ideal electrical circuit having condenser, the charging current is 90° out of phase with applied voltage. In vector notation the total current is the sum of charging current and loss current. The angle δ between the vector for the amplitude of total current and that for the amplitude of charging current is known as the loss angle. The tangent of the loss angle can be expressed as

$$\tan \delta = \frac{\text{loss current}}{\text{charging current}} = \frac{\epsilon''}{\epsilon'} \dots\dots\dots(2.8)$$

where ϵ' is the measured dielectric constant of the sample and ϵ'' is the dielectric loss factor.

A complex dielectric constant therefore can be expressed as

$$\epsilon^* = \epsilon' - j\epsilon'' \quad \dots\dots\dots(2.9)$$

2.5:Theoretical Background Of Dielectric Behaviour Of Graphene

Graphene as discussed is a monolayer of carbon atoms and possesses some unique properties for which the grapheme is also called as silicon of the 21st century. The objective of this dissertation is to find out the dielectric constant or relative permittivity of graphene and how this property can be used for next generation electromagnetic devices. The dispersion relation of dielectric constant of graphene is supported by various theories. Let's start with the Maxwell's equation and how the Maxwell's equation will lead to dispersion relation of Graphene. The Maxwell's equation is

$$\begin{aligned} \vec{\nabla} \times \vec{H} &= \mu_0 \vec{J} + \mu_0 \frac{\partial \vec{D}}{\partial t} \\ &= \mu_0 \sigma \vec{E} + \mu_0 \epsilon \frac{\partial \vec{E}}{\partial t} \quad (\because \vec{J} = \sigma \vec{E} \text{ and } \vec{D} = \epsilon \vec{E}) \end{aligned}$$

$$\text{Let } \vec{E} = E_0 e^{-i\omega t}$$

$$\Rightarrow \frac{\partial \vec{E}}{\partial t} = -i\omega \vec{E}$$

Then, $\vec{\nabla} \times \vec{H} = \mu_0 \sigma \vec{E} - i\omega\mu_0\epsilon\vec{E}$

$$\vec{\nabla} \times \vec{H} = -i\omega\mu_0 \left[\epsilon - \frac{\sigma}{i\omega} \right] \vec{E}$$

$$= -i\omega\mu_0 \left[\epsilon + \frac{i\sigma}{\omega} \right] \vec{E}$$

$$= -i\omega\mu_0 \tilde{\epsilon} \vec{E} \quad \text{Where } \tilde{\epsilon} = \left[\epsilon + \frac{i\sigma}{\omega} \right] \dots\dots\dots(2.10)$$

Graphene oxide is a monolayer of graphite oxide which consists of different functional groups like carbonyl, carboxyl, hydroxyl, epoxy. All functional groups are polar groups. The high dielectric constant of GO at low frequency has contribution from three different reasons

a.PRESENCE OF VARIOUS POLAR GROUPS

As shown in figure GO structure shows a presence of 4 polar groups like carbonyl, carboxyl, hydroxyl, epoxy. When the GO is exposed to external electric field all polar groups experience torque and orient in the direction of external electric field. This is known as orientation polarization which increases the dielectric constant.

b.PRESENCE OF DIRAC FERMIONS

A single layered graphene consists of a mono layer of carbon atom packed in 2D honeycomb lattice, with lattice constant 0.142nm. There is SP² hybridization involving 2S, 2P_x, 2P_y in XY plane. The SP² hybridized orbitals make 120⁰ with each other. The honeycomb lattice consists of six σ bonds. The remaining 2P_z orbital is perpendicular to the XY plane and make bond. Each two P_z orbitals have one electron and hence the bond is half filled. The half-filled bands play an important role in the physics of

strongly co-related bond because of their strong tight binding character and large Coulomb energy.

The energy band of a single layered graphene from the electron is

$$E_{\pm}(K) = \pm t\sqrt{3 + f(k)} - t'f(k)$$

t =nearest neighbor hopping energy

t' =next nearest neighbor hopping energy

$f(k)$ is a function given by

$$2 \cos(\sqrt{3}k_y a) + 4 \cos\left(\frac{\sqrt{3}}{2} k_y a\right) \cos\left(\frac{3}{2} k_x a\right) \dots (2.11)$$

Solving the equations we get two bands E_+ And E_- . E_+ is known as upper band or π^+ band. E_- band is known as lower band or π^- band. The lower band is completely filled and the upper band is completely empty. The two band touch each other at certain points known as Dirac points.

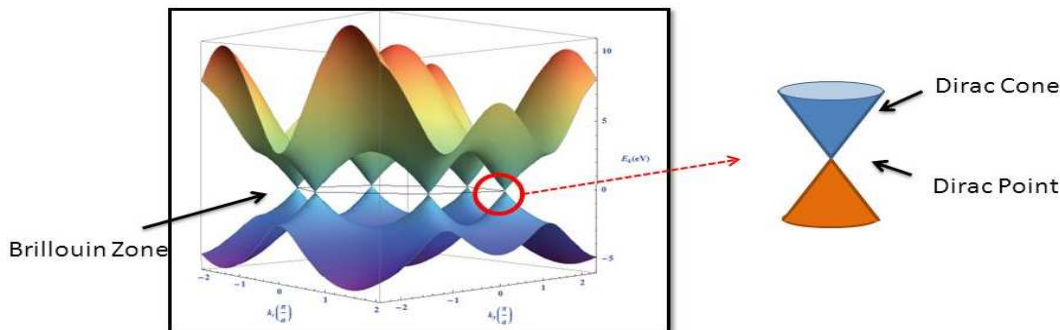


Fig 2.5: Dirac Points and dirac fermions

c.SURFACE PLASMON RESONANCE

Oscillation simply represents back and forth swing of an object induced by a driving factor either outside or inside. This behavior is observed in nearly all materials starting from vast universe to

tiny molecules . Among various oscillations electromagnetic oscillations has been paid greatest attention in the recent years. Electrons in graphene behave like Dirac fermions which are assumed massless. Due to the presence of Dirac fermions, the GO possesses extraordinary properties such as ultra high conductivity and long mean free path. The frequency at which Dirac fermions oscillate is called plasma frequency and plasma frequency is expressed as

$$\omega_p^2 = \frac{e^2 n_e}{\epsilon_0 m}$$

n_e = number density of Dirac fermions

The Maxwell's equation can be expressed as

$$\vec{\nabla} \times \vec{H} = -i\omega\epsilon_0 \left(1 - \frac{\omega_p^2}{\omega^2}\right) \vec{E}$$

ω = Frequency of the incoming electromagnetic wave

In the low frequency range $\omega < \omega_p$

$$\frac{\omega_p^2}{\omega^2} > 1$$

The conduction current dominates the displacement current. In the high frequency range ω is much greater than ω_p , the current is dominated by displacement current.

Relation between dielectric constant and frequency is

$$\epsilon(\omega) = \epsilon_0 \left(1 - \frac{\omega_p^2}{\omega^2}\right) \dots\dots\dots (2.12)$$

2.10:Recent advances in graphene oxides

In the recent years GO has been synthesized by variety of methods and GO is highly conducting in nature[33]It can be used as dielectric material in various applications. Reduced graphene oxide (r-GO) films were used to grow cells and showed enormous biocompatibility.[34] 60 Films formed of r-GO have shown potential even in solar cells.[20] Few reports on the dielectric study of GO/graphene based materials composites exist in the literature to increase the dielectric properties of host materials,[35]andgraphene based materials.[36] Recently, MnO₂ 65 decorated graphene nanoribbons showed superior permittivity and excellent microwave shielding properties.[37]S. Ruoff et al. showed that chlorinated r-GO can enhance the dielectric constant of r-GO/Polymer composites.[38] The low dielectric constant and ultrahigh strength graphene oxide/polyimide composite films were also reported.[39] Verdejo et al. showed that the homogeneous dispersion of GO through out the polymer matrix can effectively increase the dielectric permittivity.[40]Graphene-poly(vinylidene fluoride)composites with multi-layered structure prepared by a solution-cast and hot-pressing showed a large dielectric constant as high as 7940 after percolation threshold.[41]

2.11:Gap in the literature survey

Though there are a large number of papers are found in scopus about use of GO as dopant in composite materials, the dielectric study of pure GO pellets are scarce.In this view the present study will fulfill the gap.

CHAPTER 3

Chapter 3 discusses about detail experimental procedures in synthesis of GO and RGO. Different characterization techniques like XRD, FTIR, UV spectroscopy, dielectric measurements are discussed in details.

3.1 Materials :

- Graphite flakes
- Potassium permanganate (KMnO_4)
- Conc. Sulphuric acid (H_2SO_4)
- Hydrogen peroxide (H_2O_2)
- Sodium nitrate (NaNO_3) [for modified hummer's method]
- Beaker – 250 ml.
- One magnetic stirrer
- Magnetic bead
- Measuring flask
- Thermometer
- Spatula
- Funnel
- Ultrasonicator
- Ice bath set up (below 20 degree Celsius)
- Centrifuge machine
- Vacuum oven

3.2 Synthesis of Graphene Oxide (GO) By Hummer's Method

Graphene oxide was synthesized by Hummer's method through oxidation of graphite in stepwise preparation.

1. First of all a steel bowl was taken and some cold water was poured into it. The temperature was maintained below 20⁰C.

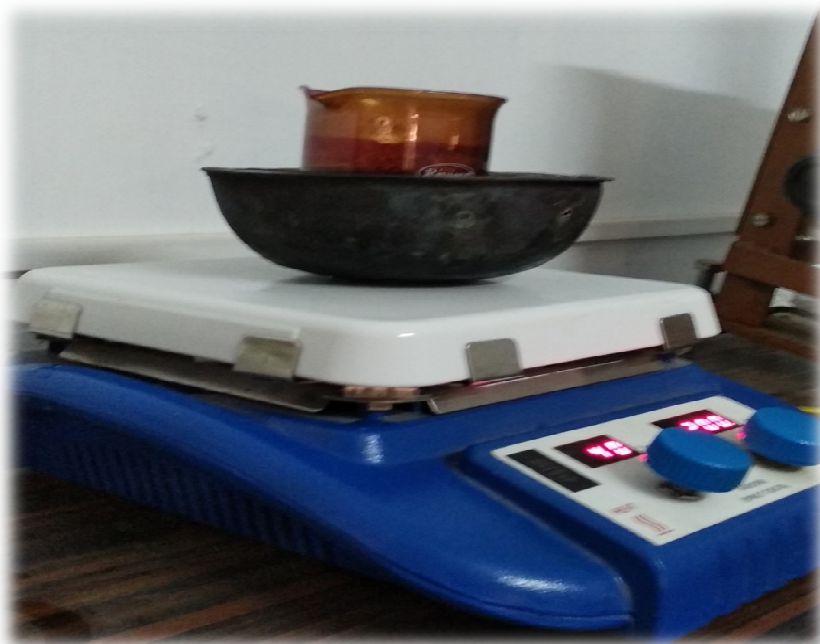


Fig 3.1 Magnetic Stirrer heating

2. Then a volumetric flask was taken and 25 ml. of concentrated sulphuric acid (H_2SO_4) was taken in it. Then 1 gm. of graphite powder with 99% of purity was added into the solution. Then 3 gm. Of potassium permanganate ($KMnO_4$) was added slowly into the solution.

3. Now the above solution was put on magnetic stirrer with rpm 200 and is continuously stirred inside the ice bath set-up (maintained below 20⁰C for 4 h).

4.The mixture was continuously stirred still the solution became pasty brownish colour .

5.Then it was diluted with slow addition of 100ml. distilled water . The reaction temperature was rapidly increased with effervescence and colour was changed to brown colour .

6.The solution was finally treated with 5ml. of hydrogen peroxide (H_2O_2) to terminate the reaction by appearance of greenish yellow



Fig 3.2 Greenish yellow colour precipitation of GO

7.Now the solution was put in the ultrasonicator for one h for purification of mixture.

8.After purification the solution was centrifuged and its pH was maintained neutral. Now the pasty GO was put in the vacuum oven for drying and then it was powdered to get the powder form of GO.



Fig 3.3 Semi liquid form of GO



Fig 3.4 Powdered GO

3.3 Reduction of GO to RGO

GO was treated with ascorbic acid and maintaining the solution at 100⁰C for 24 h .

3.4 Preparation of GO pellet

GO powder was mixed with 3%polyvinyl alcohol and thoroughly grounded. Then the ground powder was pressed with 3.5 ton load to get the desired specimen.

3.5 Characterization

The characterization of the sample aimed to obtain information of surface morphology, crystalline structure, mechanical properties and dielectric properties of Graphene Oxide . Hence, the techniques viz X-Ray diffractometer (XRD), Fourier Transform Infrared Spectroscopy (FTIR), ultraviolet Spectroscopy (UV), and dielectric properties analysis using LCR meter were employed.

3.5.1 Fourier Transform Infrared spectroscopy (FTIR)

A mixture of 5.0 mg of dried sample and 200 mg of KBr was pressed into a disk for FTIR measurement. The amount of mixture was kept constant to obtain repeatable transmission from the sample. KBr pellet is used because KBr does not absorb in the IR wavelengths between 4000- 400 wavenumbers (cm^{-1}). This way we can disperse the material usually in KBr to make a pellet. All the samples were examined by FTIR spectroscopy (FTIR Nicolet 6700/Thermofisher Scientific) using KBr pellet technique in the region 500 cm^{-1} - 4000 cm^{-1} to identify the functional groups in the samples.



Figure 3.5 Photograph of Nicolet 6700 used for obtaining FTIR spectra

3.5.2 Ultraviolet Spectroscopy (UV)

UV-visible spectral analysis of the GO powder were carried out by SHIMADZU UN 2550/JAPAN UV spectrophotometer at room temperature in the wavelength range of 240 nm to 800 nm. The sample was kept in the sample holder. The UV light source was switched on so that the light falls on the sample. The detector detected the remaining UV light that passes through the sample. The processor compared the intensity of original UV light from light source from the detected UV light. The variation of absorbance and transmittance with wavelength were recorded.



Figure 3.6 Photograph of UV 2550/SHIMADZU/JAPAN used for obtaining UV

3.5.3 Wide angle X-ray diffraction (WAXD)

Ni filtered Cu $K\alpha$ radiation having wavelength 0.1542 nm was generated at 40KV and 35 mA using WXR/SHIMADZU/JAPAN. This monochromatised X-rays were suitably collimated by passing them through slits and fall on the specimen sample which is present in the goniometer. With the help of goniometer

the angle at which the sample is positioned was measured. The detector is of high sensitivity and could detect X-rays diffracted by the sample. In this way it analyzes the orientation distribution of the crystallites present in the sample.

The X-ray diffractograms were recorded from Bragg angle 10° to 80° at room temperature of 28°C by goniometer. The goniometer was equipped with scintillation counter at a scanning speed of $10^{\circ}/\text{minute}$. The X-ray diffractograms show the variation of intensity with braggs angle



Figure 3.7 Photograph of XRD/SHIMADZU/JAPAN used for obtaining X-ray diffractogram

3.5.4 Dielectric Properties

Rectangular shaped specimens of 1cmx 1cmx 1mm were used. The rectangular surfaces of the test samples were coated with conductive silver paint. The test samples were fixed between two electrodes and kept inside the sample holder.

The capacitance and dielectric loss measurements in this study were performed by using a computer interfaced LCR HIOK/ 3532-50, JAPAN. Two sets of measurements were carried out: One is from room temperature around 26°C to 100°C at various frequencies with a heating rate of 2°C/min and another is from 1Hz to 1MHz frequency at various temperatures for the evaluation of dielectric properties of GO.

Chapter 4

RESULTS AND DISCUSSION

This chapter 4 is devoted for the characterization of prepared GO pellets by various analytical techniques such as UV-Visible spectroscopy, powder X-ray diffraction(XRD), fourier transform infrared spectroscopy(FT-IR) and the obtained results are discussed in details. This chapter also enumerates about dielectric studies of GO, variation of dielectric constant, dielectric losses, ac conductivity with variation in frequency are discussed with proper reasoning.

4.1 XRD of GO

XRD is an important characterization technique for characterization of GO. XRD pattern of GO is presented in fig4.1. As shown in fig 4.1, XRD pattern of GO exhibits a unique peak at 2θ value of 9.178° .

It corresponds to (001) reflection plane of material. The inter planar spacing (d) is 9.62784\AA . The full width half maximum(FWHM) is found to be 0.284° .

< Group: Standard Data: GO_220119 >

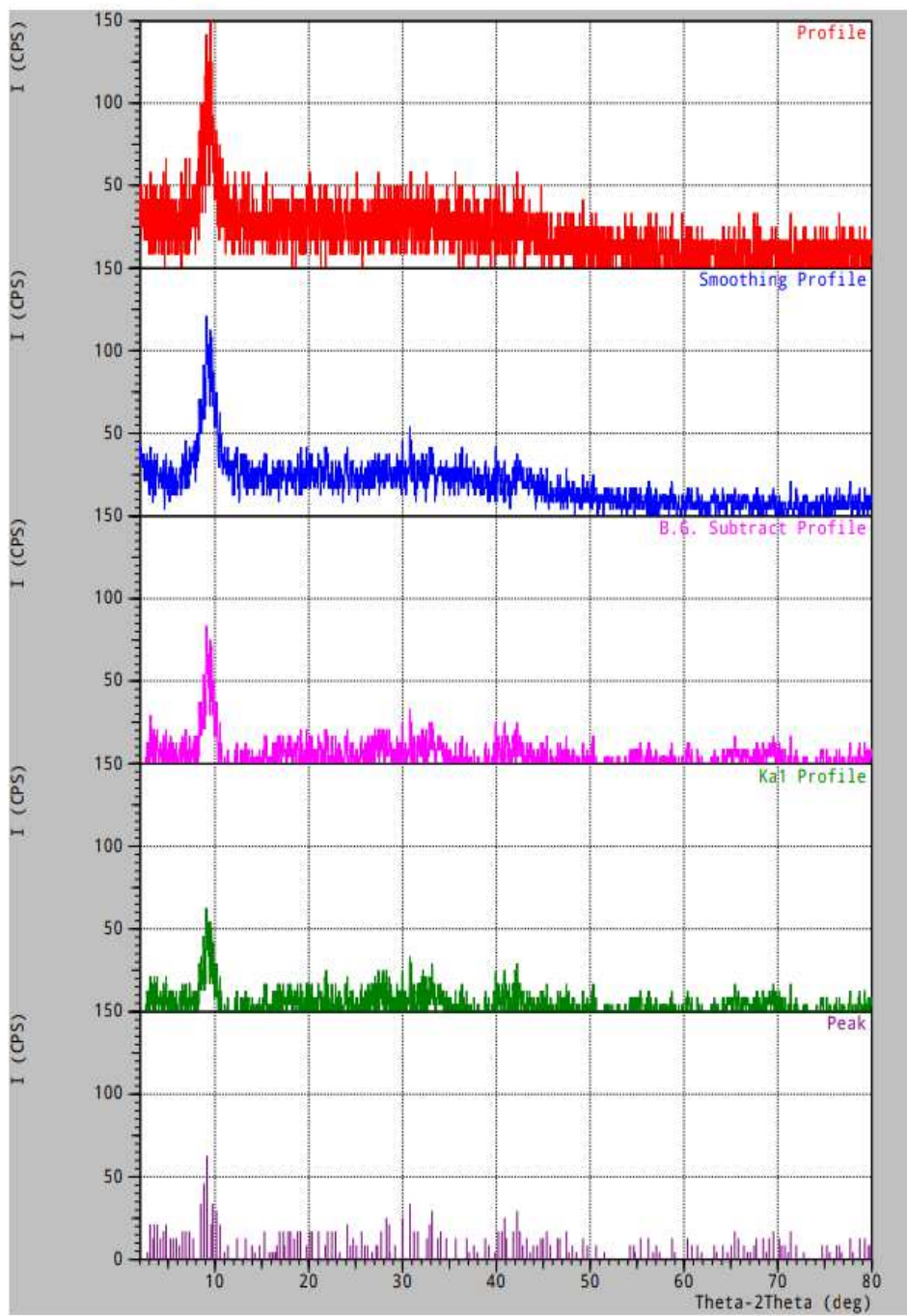


Fig 4.1: XRD of GO

4.1.1 Calculation Of Crystallite Size

Particles in a material are present as a single crystal or an agglomeration of several crystals present in a particle. Thus the particle size is usually bigger than crystalline size.

The GO was prepared in powder form during synthesis process. For powdered sample the size of crystallite form is given by Debye Schererr formula. The sharp peak observed in fig4.1 indicates the crystalline shape of GO. The broad peak indicates amorphous nature. The observed interplanar spacing in GO (9.62784 \AA^0) is more than standard interplanar spacing of graphite (3.54 \AA^0). The increased interplanar spacing in GO is due to presence of diferent functional groups.

Debye schererr formula is given as

$$D = \frac{K\lambda}{\beta \cos\theta}$$

Where K-Shape factor

λ - wavelength of incident beam

β - Full width half maximum

θ - angle of refraction

For spherical particle, shape factor is chosen as 0.9, wavelength of incident beam as 1.5 \AA^0 .

The crystal size obtained using Debye schererr formula is 27.34 nm at 9.178^0 but crystallite size is however different from particle ,the particle size is larger than crystallite size.

The particle size is measured by TEM, SAXS.

4.1.2 XRD of Reduced graphene oxide (RGO)

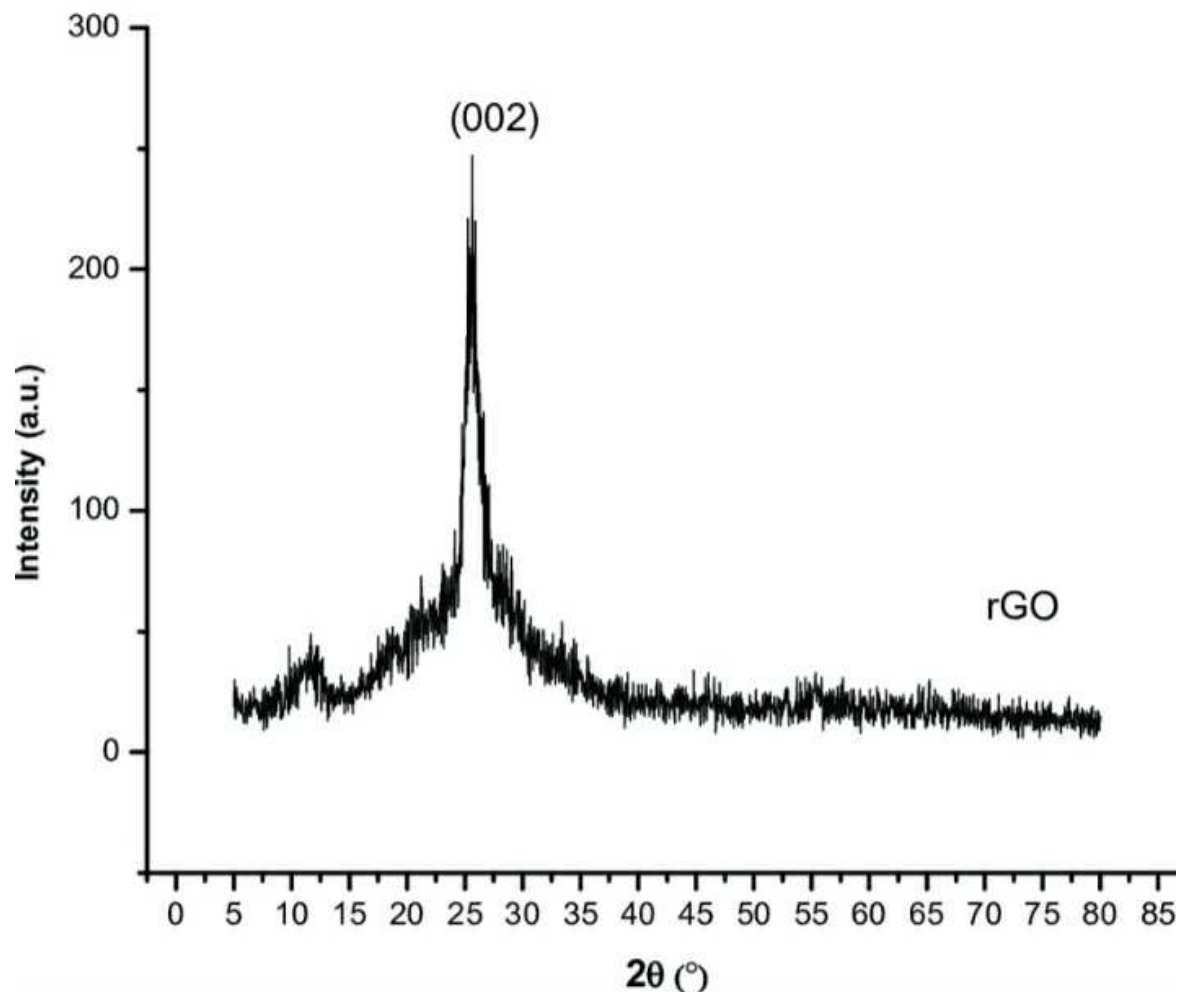


Fig:4.2: XRD pattern of RGO

The XRD of RGO is shown in fig 4.2, as observed in the XRD pattern the peak of GO at 9.178° disappears for RGO. The removal of this peak from XRD pattern confirms the removal of the functional groups present in GO. The peak at around 9.178° in GO is replaced by a less intense and broad peak at 26° . It corresponds to 002 reflection plane for RGO. The interplanar spacing obtained for RGO is 3.84\AA .

The interplanar spacing in RGO is reduced due to the removal of the oxygen functional group. Further due to absorption of moisture from the surrounding in GO the interplanar spacing is more.

The peak position 'd', FWHM and crystallite size are presented in tabular form in table1.

Table 1:Crystallography comparison of GO and RGO

Sample	Peak position	d Spacing	FWHM	Crystallite size
GO	9.1780 ⁰	9.627A ⁰	0.284 ⁰	27.34nm
RGO	26 ⁰	3.84A ⁰	0.546 ⁰	9.82nm

The increase in FWHM of RGO leads to decrease of crystallite size .The small crystallite size of RGO compared to that of GO underlines the increase in amorphous nature of RGO.

4.2 FTIR Spectra of GO

FTIR spectra of GO is shown in fig 4.3 .The specimen of GO contains numerous functional groups. The strong band at 3275.97cm⁻¹ is assigned due to –O-H stretching vibrations in the absorbed water molecules . The bands at 1638.96cm⁻¹ and 1089.94cm⁻¹ present –C-O stretching vibrations of carboxylic acid and carbonyl group respectively. All FTIR peaks and corresponding assignments are presented in table-2

Table -2:FTIR assignments

Sl No.	Wave numer	Assignment
1	3275.97	O-H Stretching

		vibration
2	1638.96	C-O stretching vibration from carboxylic
3	1089.94	C-O stretching vibration

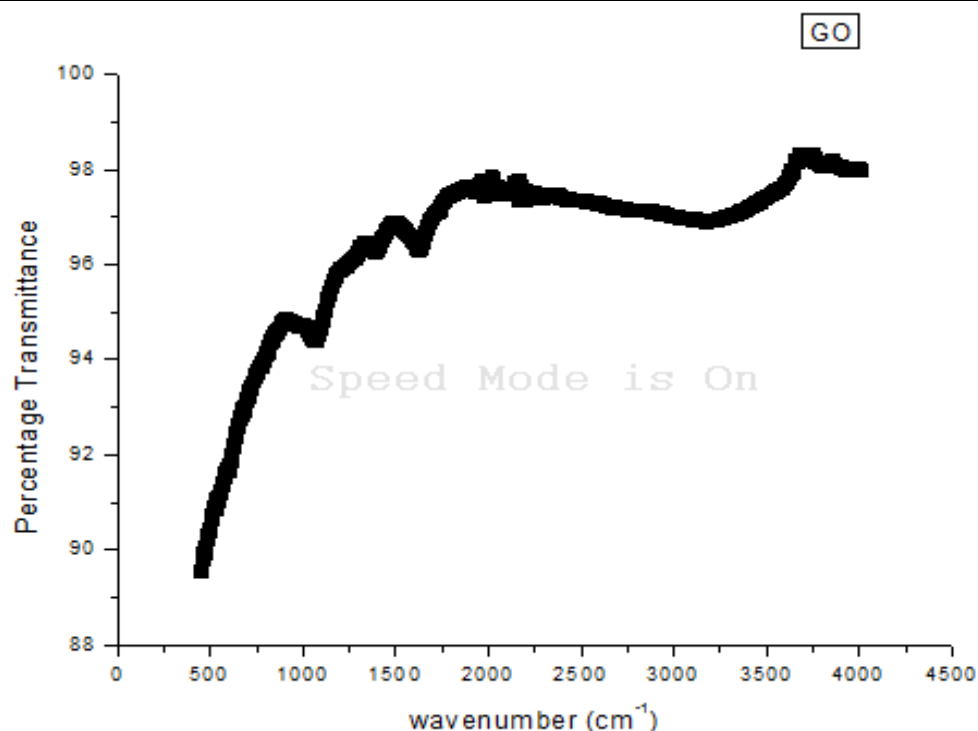


Fig 4.3 FT-IR spectrum of GO

The functional groups are at 1638.96 cm^{-1} and 1089.94 cm^{-1} testify the presence of oxygen containing functional groups.

However when the FTIR spectrum of RGO is obtained the percentage of transmittance is reduced and the absence of peaks at 1638.96 cm^{-1} and 1089.94 cm^{-1} testifies the removal of these peaks, fig 4.4 represents the FTIR spectrum of RGO.

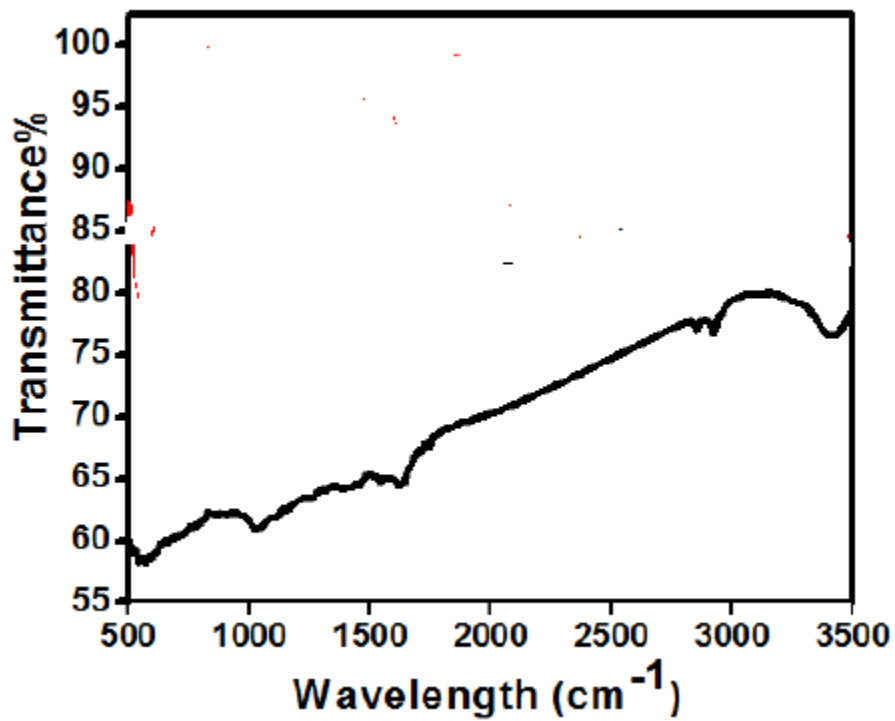


Fig 4.3 FT-IR spectrum of RGO

A low intensity band observed at 955cm^{-1} in RGO can be ascribed to C-O stretching vibrations of carbonyl group after reduction

4.3 Ultra Violet Spectra Of GO

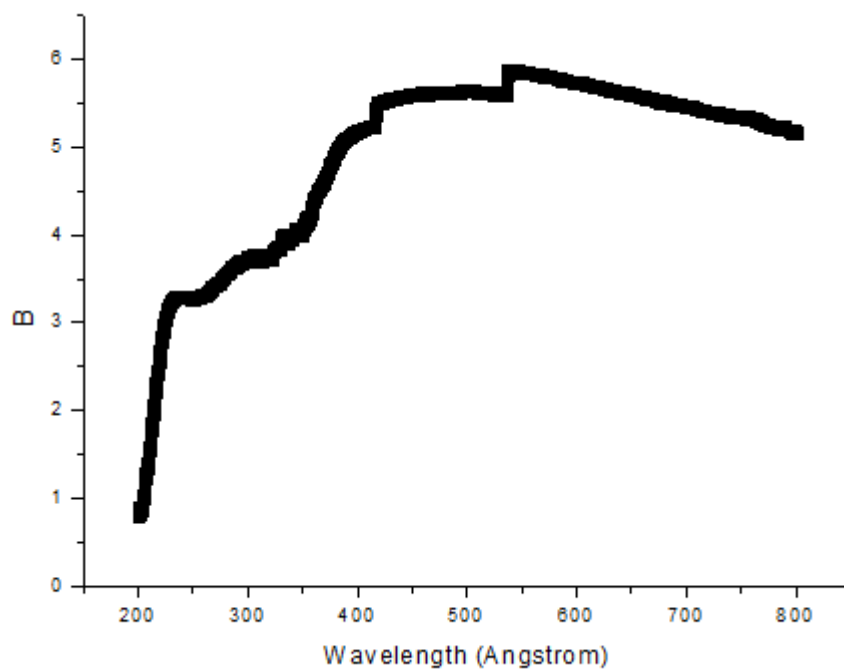


Fig 4.5 : U-V visible spectra of GO

The U-V visible light scanning wave length ranges from 200nm to 1000nm. The UV visible spectra of GO exhibits a prominent peak at 230nm . The peak at 230 nm arises due to π - π^* transition of aromatic C-C bond. The visible peak at 277nm arises (π - π) transition of aromatic C-C bonds and C=O bonds.

Therefore the GO powder is a UV absorber for wave length 230nm.

4.4 Study Of Dielectric Behaviour

Dielectric measurements were conducted for GO pellets to study its relaxation behaviors. Measurements were conducted with varying frequency from low frequency of 1 Hz to high frequency 1 MHz at room temperature of 35 °C and then varying temperature from 30 °C to 100°C at fixed frequency of 1Hz and 1KHz.

Dielectric dispersion is the dependence of permittivity of a material on the frequency of an applied electric field. There is a lag between changes in polarization and changes in electric field. Thus permittivity is a complicated function of frequency of electric field. Dielectric relaxation is the lag in dielectric constant of a material . It is analogous to hysteresis in changing magnetic field .

4.4.1 Variation of dielectric constant of GO at low frequenc

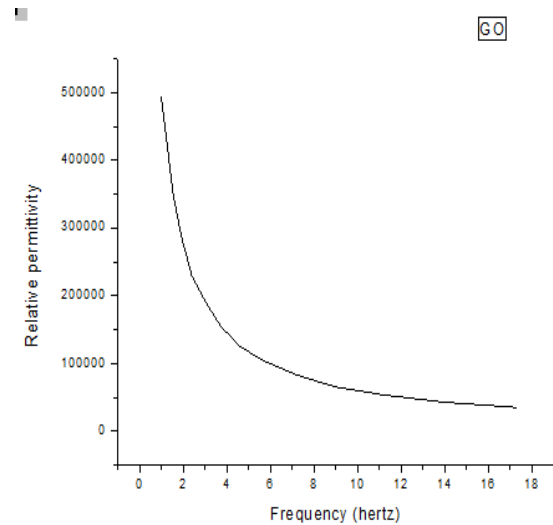


Fig 4.6(a):Variation of dielectric constant in low frequency domain

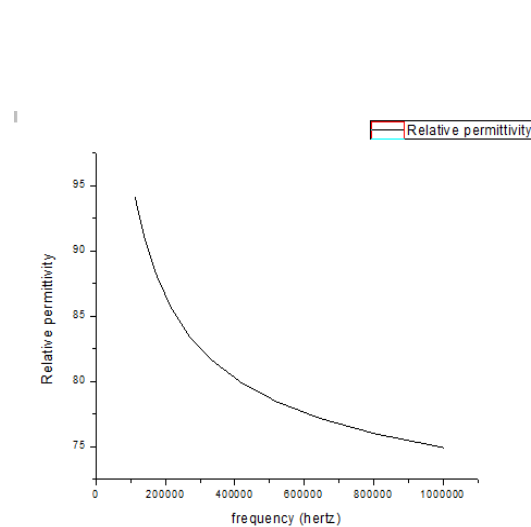


Fig 4.6(b):Variation of dielectric constant in high frequency domain

The frequency dependence of the relative permittivity known as dielectric constant is depicted in fig 4.6 .The fig 4.6(a) shows the variation of ϵ_r in low frequency range spanning from 1 Hz to 20 Hz . At low frequency of 1 Hz the dielectric constant is very high i.e. 5×10^5 . As the frequency increases dielectric constant decrease to 5000 at 20 Hz .This is an important result obtained from the experiment , because

of evolution of gigantic dielectric constant material. It is comparable to materials like $\text{CaCu}_3\text{Ti}_4\text{O}_{12}$ (10^5) and higher than various ferro electrics and perovskite titanates (1000-50000). This high dielectric constant of GO is due to various facts such as

- a) Presence of massless dirac fermions which are equivalent to electrons in metals
- b) Presence of surface plasmon resonance
- c) Presence of various functional group contributing for high orientation polarization due to their polar nature
- d) Presence of high interfacial polarization (IP). The IP is due to accumulation of unbounded charges at the interface leading to formation of large dipole.

In the low frequency region , a sudden fall of dielectric constant is observed . ϵ_r falls from 5×10^5 at 1 Hz to 1×10^5 at 20Hz. As frequency increases , some of the contributions to polarisation , such as ionic polarization , orientation polarization decreases. With increase of frequency the time interval decreases and not much time is left for polar groups to realign with external field . Thus lag increases with increase of frequency and contribute for decrease of dielectric constant.

Fig 4.6(b) depicts variation of dielectric constant from 0.2 MHz to 1MHz where dielectric constant decreases from 95 to 75 . If we compare fig 4.6(a) and in fig 4.6(b) , it is observed that there is no sudden fall of dielectric constant as observed in fig 4.6(a) . Here the decrease of ϵ_r is slow . The dielectric constant of GO is 75 even at frequency of 1MHz and it opens up many applications of GO.

4.4.2 VARIATION OF DIELECTRIC CONSTANT WITH TEMPERATURE

Fig:4.7 gives the variation of dielectric constant with temperature at low frequency 1Hz . It is observed that at 30°C the dielectric constant of GO at 1Hz is 7×10^5 . The figure depicts that dielectric constant of GO increases with increase in temperature initially upto a certain temperature and then decreases with increase in temperature. At frequency 1Hz dielectric constant increases from 7×10^5 at 30°C to 15×10^5 at 70°C and then falls to 3×10^5 at 90°C.

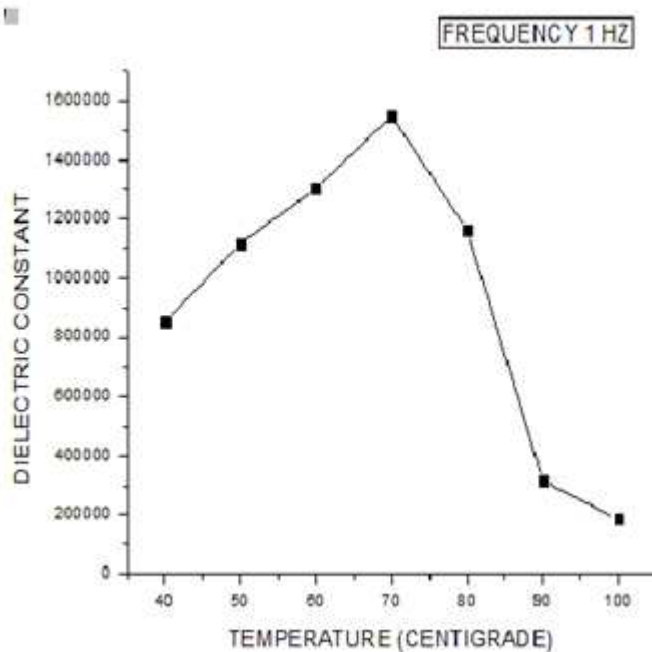
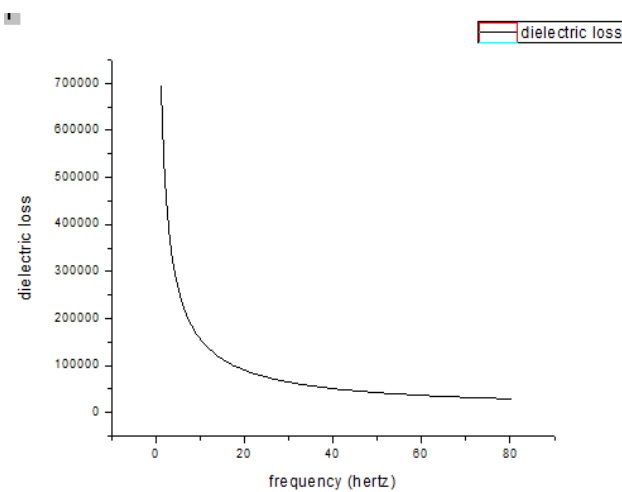


Fig 4.7: Variation of dielectric constant with temperature.

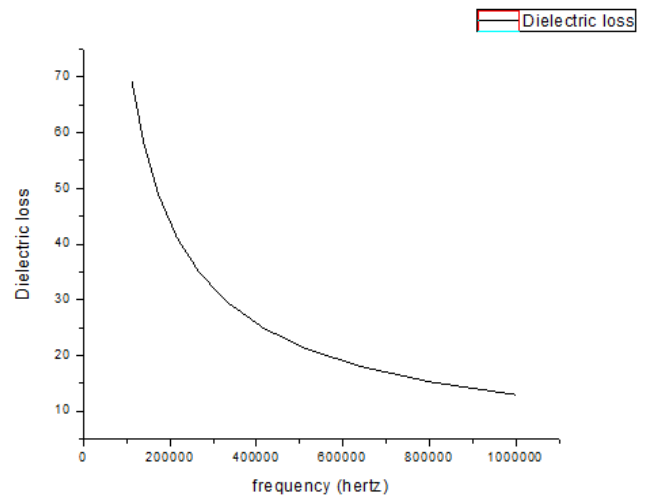
There is an obvious question why the dielectric constant of GO initially increase with temperature at particular frequency. This is due to the reorientation and rearrangement of the polarisation of the functional groups present in GO.

However increase of dielectric constant with temperature is more vigorous in low frequency region. The temperature at which dielectric constant starts decreasing is known as transition temperature. The transition temperature at 1Hz is 70°C. With rise of temperature beyond the transition temperature the chemical bonds vibrate thermally and there will be decrease in dipole moment and orientation polarisation of the functional groups. The dipoles cannot orient at high electric field and at high temperature due to higher thermal energy leading to decrease in dielectric constant at high temperature. Further at certain high temperature, there will be no moisture with vaporization of functional groups containing oxygen like -OH groups. The decrease in number of polar groups at high temperature leads to decrease of dielectric constant.

4.4.3 Variation of dielectric loss with Frequency



4.8(a) Low frequency vs. dielectric loss



4.8(b) High frequency vs. Dielectric loss

Fig 4.8(a) and fig 4.8(b) depicts the variation of dielectric loss with frequency in low frequency and high frequency domain respectively. It is observed from Fig 4.8(a) and fig 4.8(b), that dielectric loss (ϵ'') shows

similar behaviour with ϵ' . ϵ'' decreases with frequency with increase of frequency in low frequency domain and high frequency domain.

The oscillating electric field polarize the GO. This creates a dipole that also oscillates. The dipole absorbs and then reoriented or scattered in the electric field. The dipoles' responses to external field is always lagging by a certain phase. The polarizable molecules spend energy in changing the dipole orientation. When frequency of oscillating electric field resonates with frequency of oscillation of dipoles, the dipole absorbs energy and a peak is observed.

It is observed that dielectric loss is high in the low frequency domain and also the fall of dielectric loss is sudden in the low frequency domain. In the high frequency domain the dielectric loss falls but slowly as compared to low frequency region. The current in dielectric is initially displacement current at low frequency but later this is conduction current in high frequency region. When conduction current flows, it generates heat energy. We know

$$\frac{J_D}{J_C} = \frac{\epsilon\omega}{\sigma}$$

With increase of frequency, J_D (displacement current) increases, J_C (conduction current) decreases and hence loss decreases.

$$J_c = \sigma E, J_d = \epsilon(\partial E / \partial t) = \epsilon\omega E$$

4.4.4 Tan delta variation with frequency

Tan delta function is defined as ratio of dielectric loss to

dielectric constant . $\tan \sigma = \frac{\epsilon''}{\epsilon}$

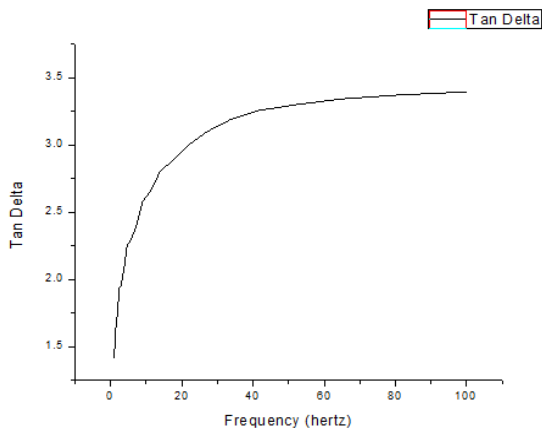


Fig4.8(a):Variation of $\tan \sigma$ in low frequency domain

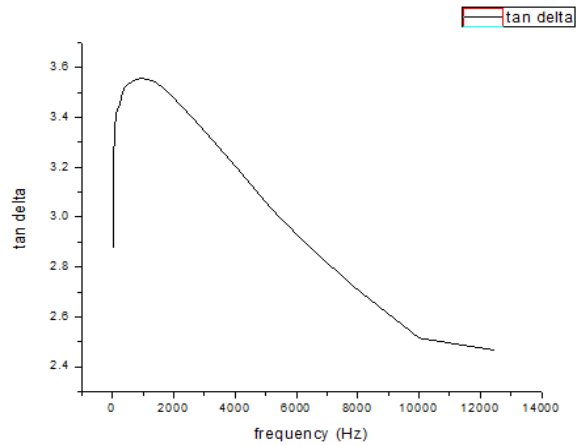


Fig 4.8(b)Variation of $\tan \sigma$ in mid frequency domain

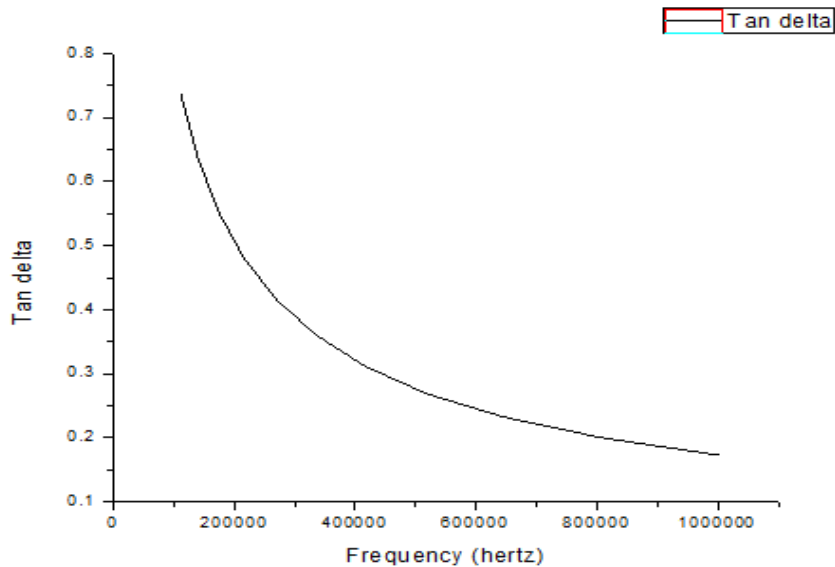
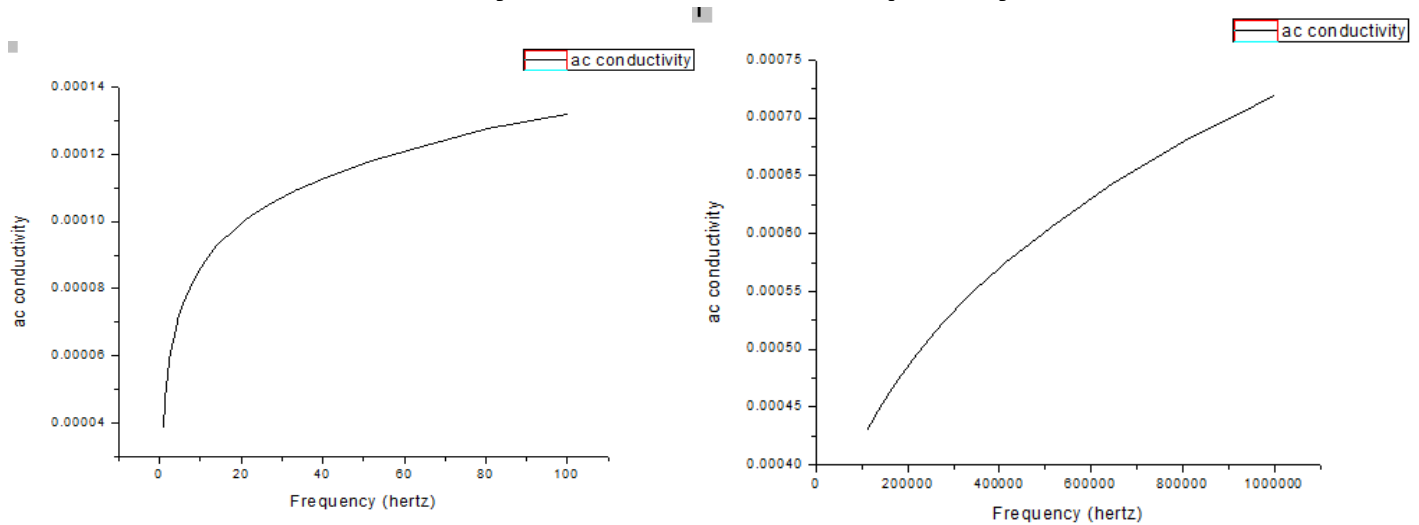


Fig 4.8(c)Variation of $\tan\sigma$ in high frequency domain

Fig 4.8 (a),(b),(c) depicts the variation of $\tan\sigma$ in the low frequency range , mid frequency range , and high frequency range respectively .In the low frequency region as shown in fig 4.8(a) , the $\tan\sigma$ increases with increase of frequency . In the low frequency region both dielectric constant and dielectric loss are high. However the change in dielectric loss is more compared to the change in dielectric constant. Therefore $\tan\sigma$ increases with increase of frequency and suffers a transition at 1.39×10^3 Hz. Beyond this frequency $\tan\sigma$ decreases with increase of frequency. Then at high frequency both dielectric loss and constant are minimum leading to decrease of $\tan\sigma$.

4.4.5 AC conductivity variation with frequency



[Fig4.9(a)low frequency variation vs conductivity] [Fig4.9(b)high frequency vs conductivity]

DC conductivity is determined only by resistance.

$$\sigma_{dc} = \frac{l}{RA}$$

but ac conductivity depends on skin depth i.e. the thickness in conducting material upto which the amplitude of electromagnetic wave decreases to $1/e$. The ac current flows only at the skin of the conductor.

$$J = j_s \exp\left(-\frac{d}{\lambda}\right)$$

J_s is the current density at surface and J is the current density at depth 'd'.

λ = skin depth

$$\lambda = \sqrt{2\rho/\omega\mu}$$

With increase of ω , λ decreases, $\frac{d}{\lambda}$ increases, J_c decreases.

Now σ_{ac} is given by

$$\sigma_{ac} = \epsilon_r (\tan\delta) \omega \epsilon_0$$

$$\sigma_{ac} = \epsilon'' \omega \epsilon_0 \dots \dots \dots (4.1)$$

$$\sigma_{ac} = \sigma_0 \exp(-E_a/KT)$$

As frequency increases more and more of bound charges start to oscillate out of phase with applied voltage. This contribute to increase the ac conductivity with increase of frequency. ac conductivity increases from $0.00004 \text{ohm}^{-1} \text{cm}^{-1}$ at 1 Hz to 0.00075 at 1MHz.

4.4.6 Cole cole plot

Cole cole plots are indicator of relaxation present in a material. These are plotted by taking imaginary part of relative permittivity i.e dielectric loss on y axis and real part i.e dielectric constant on x axis. The variation of dielectric loss and dielectric constant with frequency are governed by Debye equation.

$$\epsilon'(\omega) = \epsilon_\infty + \frac{\epsilon_s - \epsilon_\infty}{1 + \omega^2 \tau^2}$$

$$\epsilon''(\omega) = \frac{(\epsilon_s - \epsilon_\infty) \omega \tau}{1 + \omega^2 \tau^2}$$

.....4.2

Equation 4.2 are known as Debye expression and gives frequency dependence of both dielectric constant and

dielectric loss. The material that obeys Debye's relation will have a Cole-Cole plot like a perfect semicircle. And for materials not obeying Debye's laws or whose dielectric loss does not show any relaxation, Cole-Cole plots are not semicircles. Fig 4.10 gives the Cole-Cole plot for GO keeping frequency as the varying parameter.

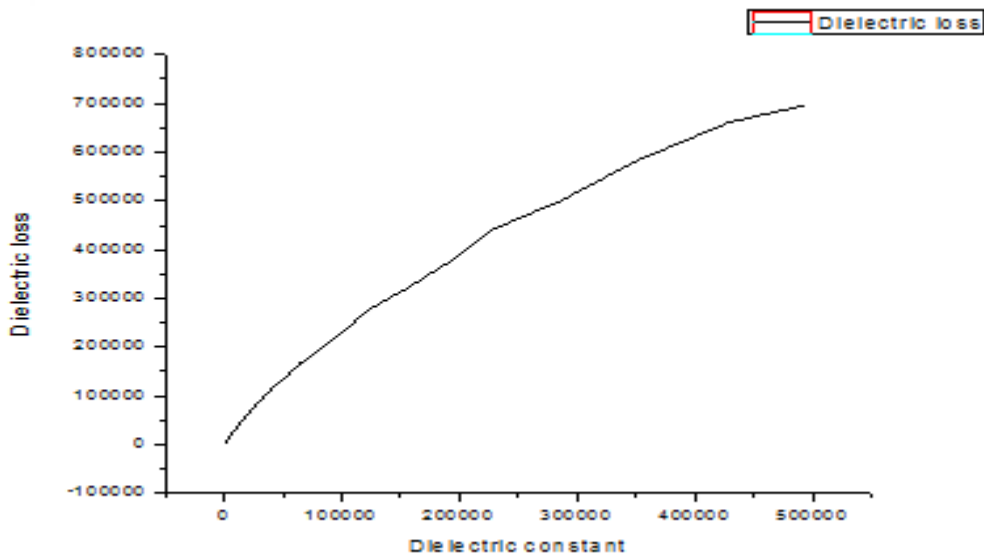


Fig 4.10: Cole Cole plot for GO

As there is no relaxation observed in the imaginary part of dielectric constant as shown in fig 4.8 in both low and high frequency domain, Cole-Cole plots are not semicircles having no relaxations. GO does not obey Debye's relaxation.

Chapter 5

Conclusion

Graphene oxide and reduced graphene oxide pellets were prepared by Hummers Method. The FTIR spectra revealed the removal of functional groups namely epoxide groups, carbonyl group, carboxyl and hydroxyl groups from GO. The XRD analysis hinted the conversion of Graphene oxide to Graphene as indicated by the disappearance of characteristic peak of Graphene Oxide. The dielectric behaviour of GO was studied with variation in frequency and variation in temperature with special reference to effect of -OH and -COOH functional groups which are responsible for the change in polarization of GO sheet under the applied electric fields at the various temperatures and frequency... Present study strongly concluded that the novel GO exhibits very high dielectric constant and is in the order of 10^5 in magnitude and it increases still with rise of temperature but falls with increase of frequency. This value is very high, which is even very high compared to the conventional giant dielectric material such as $\text{CaCu}_3\text{Ti}_4\text{O}_{12}$ and perovskites. The reorientation/rearrangement of the attached functional groups (-OH and -COOH) in the GO resulted change in the dipole moment and the polarization which lead to the high dielectric constant at low frequency range. This newly synthesized GO with colossal dielectric constant is likely to enable us further scaling advances in performances of the electronic and energy storage devices. These GO can be used as reinforcements like dopants to synthesize composite materials of high dielectric constant. The increase the ac conductivity with increase of frequency from $0.00004 \text{ ohm}^{-1} \text{ cm}^{-1}$ at 1 Hz to 0.00075 at 1MHz suggests that the GO can be used in transmission of signals in the high frequency range.

References

1. P. Van Musschen Broek, Introduction Philosophion Naturalem, Luchtman, Leiden (1762)
2. M. Faraday, Phil. Trans 128:1 79 265 (1837)
3. O.F. Mossoti, Bibl. univ. modena 6, 193 (1847)
4. O.F. Mossoti, Mem. di Mathem e. di. fisica in modena, 24(2) 49 (1850)
5. R. Clausius Volume 2 Vieweg. Braunschweig (1879)
6. P. Debye, Phys. Z, 13, 97 (1912)
7. L. Onsager, J. Amer. Chem. Soc, 58, 1486 (1936)
8. J.G. Kirkwood J. Chem. Phys, 7, 911 (1939)
9. J.G. Kirkwood and R.M. Fuoss, J. Chem. Phys, 9, 329 (1941)
10. P. Drude, Z. phys. Chem, 23, 267 (1897)
11. K.S. Cole and R.H. Cole, Journal of Chemical phys, 9, 341 (1941)
12. D.W. Davidson and R.H. Cole. J. Chem. Phys, 19, 1484 (1951)
13. G. Williams and D.C. Watt Trans Faraday Soc, 66, 80 (1970)
14. A.K. Jonscher, Dielectric relaxation in solids, Chelsea dielectric press, London (1983)
15. R. Chau, J. Brask, S. Datta, G. Dewey, A. Majumdar Microelectronic Engineering 80, 1 (2005)

16. P.P.Jenkins, A.N.Maclnnes, M.Tabib Azar and A.R.Barron, *Science* 263, 1751(1994)
17. B. J. Li, H. Q. Cao, J. Shao, M. Z. Qu and J. H. Warner,, *J.Mater. Chem.*, , 21, 5069(2011)
18. S. Dubin, S. Gilje, K. Wang, V. C. Tung, K. Cha, A. S. Hall, J.Farrar, R. Varshneya, Y. Yang and R. B. Kaner, *ACSNano*, 4, 3845(2010)
19. S. Xu , L .Yong, and P. Wu, *ACS Appl. Mater. Interfaces*, 5, 654(2013)
20. K. P Loh, Q. L. Bao, G. Eda and M. Chhowalla, *Nat. Chem.* 2, 1015(2015)
21. Y. Hernandez, V. Nicolosi, M. Lotya, F.M Blighe and Z.Y. SunDe, *Nat Nanotechnol.*, , 35, 63.(2008)
22. V. G. Kozlov, V. Bulovic, P. E. Burrows, S. R. Forrest,*Nature*, , 389 362.(1997)
- 23.T. Förster , *Discuss Farady Soc.* ,27, 7(1959)
24. D. M. Willard, L. L. Carillo, J. Jung and A. V. Orden, *NanoLett.*, 1, 469.(2001)
25. Jares- Erijman, E. A., and T. M. Jovin, *Nat. Biotechnol.*21,1387(2003)
26. S .Stankovich, D. A. Dikin, R. D. Piner, K. A. Kohlhaas, A. Kleinhammes, Y.Y Jia, Y .Wu, S. B. T Nguyen and R.S Ruoff *Carbon*, 45,1558(2007)
27. M. Qian , T. Feng, H. Ding, L. F. Lin, H. B.Li, Y.W. Chen andZ. Sun *Nanotechnology* , 20, 425702(2009).
28. J. Nishijo, Ch. Okabe, O. Oishi and N. Nishi, *Carbon*, 2943–2949.(2006)
- 29.R. Sergiienko, E. Shibata, Z. Akase, H. Suwa, T. Nakamura and D. Shindo, *Mater.Chem. Phys.* 98, 34.(2006)
30. K. Morishige and T. Hamada, *Langmuir* , , 21, 6277(2005)
31. M. Bystrzejewski, S. Cudzilo, A. Huczko, H. Lange, G. Soucy, G. Cota-Sanchez, W. Kaszuwara, *Biomol. Eng* 24, 555.(2007)
- 32.K Santosh kumar, Suresh Pittala,RSC Advances, 23,65(2018)

33. H. Chen, M. B. Müller, K. J. Gilmore, G. G. Wallace, and D. Li, *Adv. Mater.*, 20, 3557–3561. (2008)
34. Y. Bai, Y. Cao, J. Zhang, M. Wang, R. Li, P. Wang, S. M. Zakeeruddin, and M. Gratzel, *Nat Mater*, 7, 626–630. 95 (2008)
35. Ramanathan T., A. A., Stankovich S., D. A., Herrera-Alonso M., P. D., A. H., S. C., Chen X., R. S., N. T., A. A., P. K., and B. C., *Nat Nano*, 3, 327–331(2008)
36. S. Stankovich, D. A. Dikin, G. H. B. Dommett, K. M. Kohlhaas, E. J. Zimney, E. A. Stach, R. D. Piner, S. T. Nguyen, and R. S. Ruoff, *100 Nature*, 442, 282–286(2006)
37. T. K. Gupta, B. P. Singh, V. N. Singh, S. Teotia, A. P. Singh, I. Elizabeth, S. R. Dhakate, S. K. Dhawan, and R. B. Mathur, *J. Mater. Chem. A* 2, 4256–4263(2014).
38. J.-Y. Kim, W. H. Lee, J. W. Suk, J. R. Potts, H. Chou, I. N. 105 Kholmanov, R. D. Piner, J. Lee, D. Akinwande, and R. S. Ruoff, *Adv. Mater.*, 25, 2308–2313(2013).
39. J.-Y. Wang, S.-Y. Yang, Y.-L. Huang, H.-W. Tien, W.-K. Chin, and C.-C. M. Ma, *J. Mater. Chem.*, , 21, 13569–13575.(2011)
40. L. J. Romasanta, M. Hernández, M. a López-Manchado, and R. 110 Verdejo, *Nanoscale Res. Lett* 6, 508. (2011)
41. P. Fan, L. Wang, J. Yang, F. Chen, and M. Zhong, *Nanotechnology*, , 23, 365702(2012)

